Journal of Medicinal Chemistry

Article

pubs.acs.org/jmc

Inhibitors of β-Site Amyloid Precursor Protein Cleaving Enzyme (BACE1): Identification of (*S*)-7-(2-Fluoropyridin-3-yl)-3-((3-methyloxetan-3-yl)ethynyl)-5′*H*-spiro[chromeno[2,3-*b*]pyridine-5,4′-oxazol]-2′-amine (AMG-8718)

Thomas A. Dineen,*[,†] Kui Chen,[§] Alan C. Cheng,[§] Katayoun Derakhchan,[⊥] Oleg Epstein,[†] Joel Esmay,[∥] Dean Hickman,[∥] Chuck E. Kreiman,[†] Isaac E. Marx,[†] Robert C. Wahl,[§] Paul H. Wen,[‡] Matthew M. Weiss,[†] Douglas A. Whittington,[§] Stephen Wood,[‡] Robert T. Fremeau, Jr.,[‡] Ryan D. White,[†,‡] and Vinod F. Patel[†,#]

[†]Departments of Therapeutic Discovery, [‡]Neuroscience, [§]Molecular Structure and Characterization, [∥]Pharmacokinetics and Drug Metabolism, and [⊥]Comparative Biology and Safety Sciences, Amgen, Inc., 360 Binney Street, Cambridge, Massachusetts 02142, and One Amgen Center Drive, Thousand Oaks, California 91320, United States

Supporting Information

ABSTRACT: We have previously shown that the amino-oxazoline xanthene scaffold can generate potent and orally efficacious BACE1 inhibitors although certain of these compounds exhibited potential hERG liabilities. In this article, we describe 4-aza substitution on the xanthene core as a means to increase BACE1 potency while reducing hERG binding affinity. Further optimization of the P3 and P2′ side chains resulted in the identification of **42** (AMG-8718), a compound with a balanced profile of BACE1 potency, hERG binding affinity, and Pgp recognition. This compound produced robust and sustained reductions of CSF and brain Aβ levels in a rat pharmacodynamic model and exhibited significantly reduced potential for QTc elongation in a cardiovascular safety model.

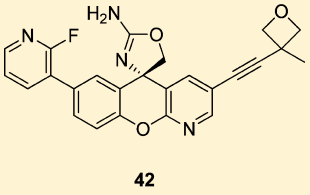

42

	42
BACE1 IC_{50} (nM):	0.7
BACE Cellular IC_{50} (nM):	4.4
Papp ($x10^{-6}$ cm/s):	19
Human / Rat Pgp ER:	5.8 / 9.2
hERG Ki (μM):	>10
logP:	2.53
PSA:	92

INTRODUCTION

Alzheimer's disease (AD) is the most common form of dementia and is characterized by cognitive decline, changes in thinking, memory loss, and ultimately death. Although AD affects over 18 million people worldwide, there are currently no available disease-modifying therapies and the available treatments provide only limited benefit.[1]

A large body of evidence has implicated the formation and accumulation of amyloid β (Aβ) peptides, specifically $Aβ_{40}$ and $Aβ_{42}$, in the brains of AD patients as critical factors in the pathogenesis of the disease.[2] Aβ peptides are formed in the brain via sequential proteolytic cleavage of amyloid precursor protein (APP) by the aspartyl proteases BACE1 (β-site APP cleaving enzyme) and γ-secretase.[3] The amyloid hypothesis suggests that inhibiting the formation and accumulation of Aβ in the brain could result in a disease-modifying effect in AD patients.[4] Recently published genetic evidence has provided further support for this approach, suggesting that even modest decreases in the formation of Aβ (as a result of a mutation in the gene encoding APP) may confer significant protection against the development of AD.[5]

Since its identification in 1999,[3] BACE1 has attracted a significant amount of attention as a potential target for the development of an AD therapy. BACE1 contains a long, shallow, and hydrophilic active site, and early efforts to identify BACE1 inhibitors produced large, polar compounds with unfavorable physicochemical properties and consequently poor pharmacokinetics and central nervous system (CNS) penetration.[6] More recently, a number of groups have described BACE1 inhibitors that employ a 2-aminoheterocycle which engages in hydrogen bonding interactions with the catalytic aspartic acid residues of the protease.[7] These heterocyclic units bind to the enzyme in an orientation that allows for further extension of a side chain into the S1 and S3 pockets. These designs have resulted in the identification of a number of potent BACE1 inhibitors with significantly improved pharmacokinetic profiles and CNS penetration compared with earlier peptidomimetic inhibitors.

Our own efforts in this area led to the discovery of the aminooxazoline xanthene scaffold,[8] which enabled extension of side chains into both the S3 and S2′ pockets of BACE1 and led to the identification of compound **1** (Figure 1).[9] While this compound led to robust reduction in central Aβ when dosed orally to Sprague−Dawley (SD) rats, its advancement was limited due to off-target activity on the hERG channel. Indeed, when evaluated in an anesthetized dog cardiovascular model, compound **1** caused prolongation of the QTc interval at

Received: August 18, 2014

   dx.doi.org/10.1021/jm5012676 | *J. Med. Chem.* XXXX, XXX, XXX−XXX

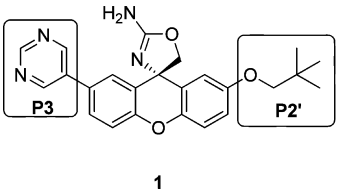

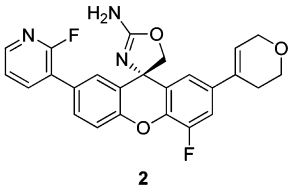

	1	2
BACE1 IC_{50} (nM):	2.2	0.3
BACE Cellular IC_{50} (nM):	25	4.1
HLM / RLM (μL/min/mg):	21 / 21	52 / 35
Papp ($x10^{-6}$ cm/s):	13	10
Human / Rat Pgp ER:	1.5 / 0.9	1.0 / 1.0
hERG Ki (μM):	0.66	3.3

Figure 1. Previous efforts to balance hERG inhibition and Pgp-mediated efflux.

Scheme 1. Synthesis of the P2′-Neopentyloxy 4-Azaxanthenes 26−28[a]

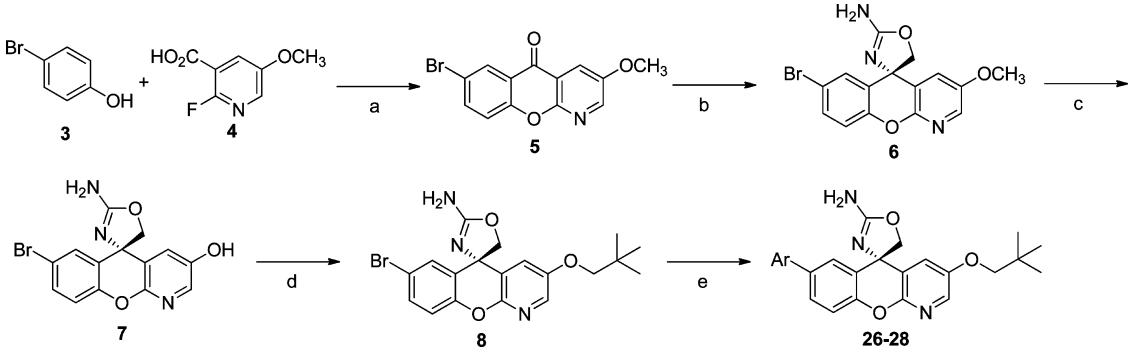

[a]Reagents: (a) (i) NaH, DMF, 130 °C, 55%, (ii) PPA, 140 °C, 93%; (b) (i) MeMgCl, THF, −30 °C, HCl/Et_2O, (ii) I_2, AgOCN, THF, −40 °C, (iii) NH_3, 23 °C; (iv) chiral SFC, 29%; (c) BBr_3, DCM, 0 °C, 51%; (d) neopentyl iodide, Cs_2CO_3, DMF, 100 °C, 63%; (e) Ar-$B(OH)_2$, $Pd(PPh_3)_4$ or $Pd(AmPhos)_2Cl_2$, K_2CO_3, THF−H_2O, 110 °C, 72−90%.

Scheme 2. Preparation of 4-Azaxanthenes via Late-Stage Installation of the P2′ Group[a]

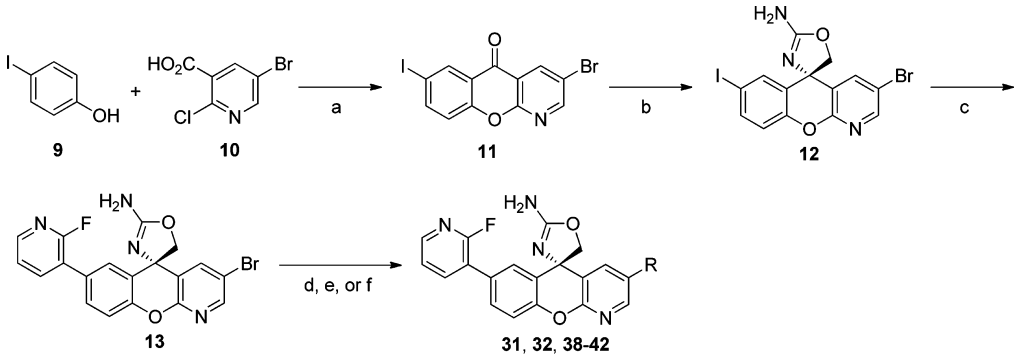

[a]Reagents: (a) (i) NaH, DMF, 130 °C, 76%, (ii) PPA, 140 °C, 85%; (b) (i) MeMgCl, THF, −30 to 0 °C, THF−$CHCl_3$, 80 °C, (ii) I_2, AgOCN, THF, −20 °C, (iii) NH_3, 23 °C, (iv) chiral SFC, 13%; (c) 2-fluoro-3-pyridineboronic acid, $Pd(dppf)Cl_2$, K_2CO_3, 1,4-dioxane−water, 70 °C, 91%; (d) R-$B(OH)_2$, $Pd(PPh_3)_4$, K_2CO_3, 1,4-dioxane−water, 80 °C, 40−59%; (e) R-CCH, $Pd(PPh_3)_4$, CuI, *i*-$PrNH_2$−DMF, 90 °C, 58−95%; (f) R-C≡C-TMS, $Pd(PPh_3)_4$, CuI, TBAF, THF, 70 °C, 89% for **42**.

relatively low exposure multiples over the in vivo EC_{50} for brain Aβ reduction in a rat pharmacodynamic model. Subsequent SAR studies demonstrated that the hERG binding affinity of these compounds could be reduced by incorporating polar heteroatoms in the P2′ region of the inhibitor, albeit at the expense of increased Pgp-mediated efflux and consequently lower CNS exposure.[10] Further fine-tuning of physicochemical properties indicated that these increases in transporter-mediated efflux could be attenuated by reducing the PSA of the P3 group and by fluoro-substitution on the xanthene ring. The incorporation of a fluorine atom at the 4-position of the xanthene ring (e.g., **2**) also resulted in compounds with improved (5−10×) BACE1 potency.[9] The increased BACE1 potency within this series was attributed to a hydrogen bonding interaction between the 4-fluoro atom and Trp76 of BACE1, as observed in crystal structures of these compounds with the enzyme.[11]

In this article, an alternative strategy is described for balancing BACE1 potency, hERG binding affinity, and Pgp-mediated efflux by incorporating a nitrogen atom into the xanthene core structure of the aminooxazoline xanthene inhibitors. Further optimization of the P3 and P2′ groups led to the identification of a metabolically stable, orally efficacious BACE1 inhibitor with a favorable balance of in vivo efficacy to off-target effects.

CHEMISTRY

The synthesis of inhibitors BACE1 inhibitors **26−28** (Table 1) is outlined in Scheme 1. Coupling of *p*-bromophenol (**3**) with 2-fluoropyridine **4** under basic conditions in DMF, followed by ring-closure of the resulting intermediate in neat polyphos-

dx.doi.org/10.1021/jm5012676 | J. Med. Chem. XXXX, XXX, XXX−XXX

Scheme 3. Synthesis of 4-Azaxanthenes 33−37[a]

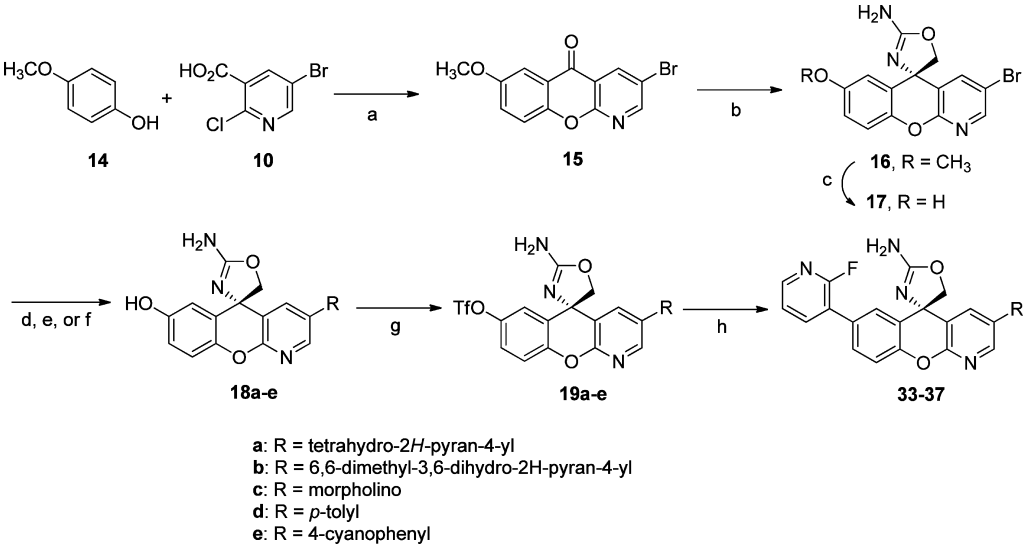

a: R = tetrahydro-2*H*-pyran-4-yl
b: R = 6,6-dimethyl-3,6-dihydro-2H-pyran-4-yl
c: R = morpholino
d: R = *p*-tolyl
e: R = 4-cyanophenyl

[a]Reagents: (a) (i) NaH, DMF, 140 °C, 83%, (ii) PPA, 140 °C, 66%; (b) (i) MeMgBr, THF, −30 to 0 °C, CH_3OH, 60 °C, 53%, (ii) I_2, AgOCN, THF, −20 °C, (iii) NH_3, 23 °C, (iv) chiral SFC, 28%; (c) BBr_3, DCM, 0 °C, 62%; (d) (i) 2-(3,6-dihydro-2*H*-pyran-4-yl)-4,4,5,5-tetramethyl-1,3,2-dioxaborolane, $Pd(PPh_3)_4$, K_2CO_3, DMF, water, 80 °C, 70%, (ii) H_2 (1 atm), 10% Pd/C, MeOH, 82% of **18a**; (e) R-$B(OH)_2$, $Pd(PPh_3)_4$ or $Pd(AmPhos)_2Cl_2$, K_2CO_3, 1,4-dioxane−water, 75−100 °C, 34−69% for **18b**, **18d**, and **18e**; (f) morpholine, $Pd_2(dba)_3$, DavePhos, LHMDS, THF, 70 °C, 51% of **18c**; (g) $PhNTf_2$, Et_3N, DCM, 67−89%; (h) 2-fluoro-3-pyridineboronic acid, $Pd(PPh_3)_4$, K_2CO_3, 1,4-dioxane−water, 80 °C, 34−97%.

Scheme 4. Synthesis of BACE1 Inhibitor 30[a]

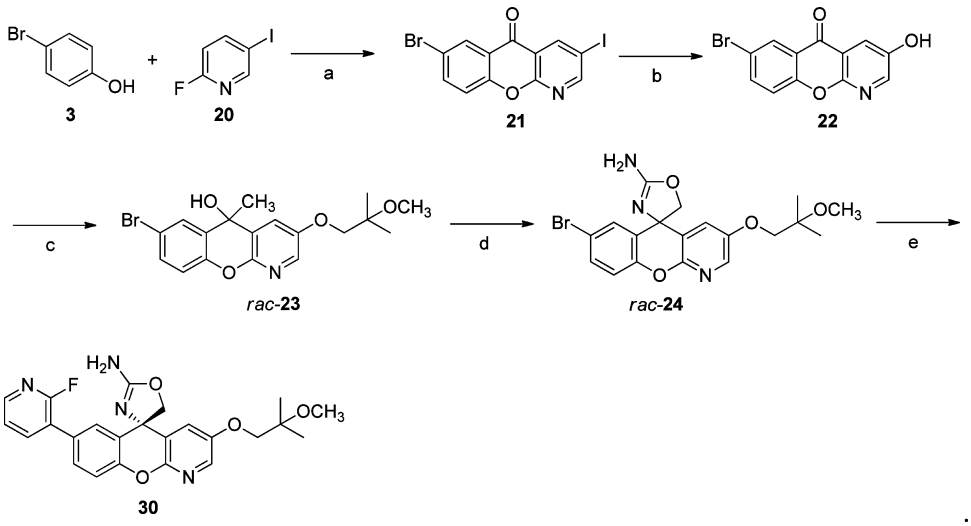

[a]Reagents: (a) (i) LiTMP, THF, −10 °C, then CO_2(g), **20**, K_2CO_3, DMF, 140 °C, (ii) PPA, 140 °C; (b) (i) $Pd(OAc)_2$, X-Phos, $B_2(pin)_2$, K_3PO_4, 1,4-dioxane, 23 °C, (ii) 30% H_2O_2, THF, 66%; (c) (i) 3-bromo-2-methylpropene, DBU, DCM, (ii) NIS, MeOH, (iii) MeMgCl, THF, −40 °C, (iv) $LiBEt_3H$, THF, 9% over four steps; (d) (i) HCl/1,4-dioxane, 50 °C, (ii) I_2, AgOCN, THF, −20 °C, (iii) NH_3, 23 °C, 16%; (e) (i) 2-fluoro-3-pyridineboronic acid, $Pd(PPh_3)_4$, K_2CO_3, THF−water, 110 °C, (ii) chiral SFC, 16%.

phoric acid, afforded xanthenone **5**. As described in the preceding article for the analogous 4-fluoroxanthenes,[9] the aminooxazoline unit was installed via a three-step sequence as follows. Reaction of ketone **5** with MeMgCl and subsequent HCl treatment afforded an unstable *exo*-olefin. The olefin was treated directly with in situ generated iodine isocyanate followed by a solution of ammonia in 2-propanol to yield the 2-aminooxazoline xanthene in racemic form.[12] Separation of the racemate through chiral supercritical fluid chromatography (SFC) afforded the (*S*)-enantiomer **6** on multigram scale. The preparation of neopentyl ether **8** was accomplished by boron tribromide-mediated demethylation of **6**, followed by cesium carbonate-promoted alkylation of intermediate phenol **7** with neopentyl iodide. Palladium catalyzed Suzuki cross-coupling reactions with the corresponding boronic acids[13] afforded the final analogues **26**−**28**.

The compounds in Tables 2 and 3 were generated via several different routes. Selected C-linked P2′ analogues (**31**, **32**, and **38**−**42**) were prepared as described in Scheme 2 via the common dihalo intermediate **12**. Coupling of *p*-iodophenol (**9**) and 2-chloropyridine **10**, followed by acidic ring closure, gave xanthenone **11**. Formation of the 2-aminooxazoline xanthene unit and chiral separation was accomplished as described above to afford the bis-functionalized iodo-bromo intermediate **12**.

dx.doi.org/10.1021/jm5012676 | *J. Med. Chem.* XXXX, XXX, XXX−XXX

Scheme 5. Synthesis of BACE1 Inhibitor 29[a]

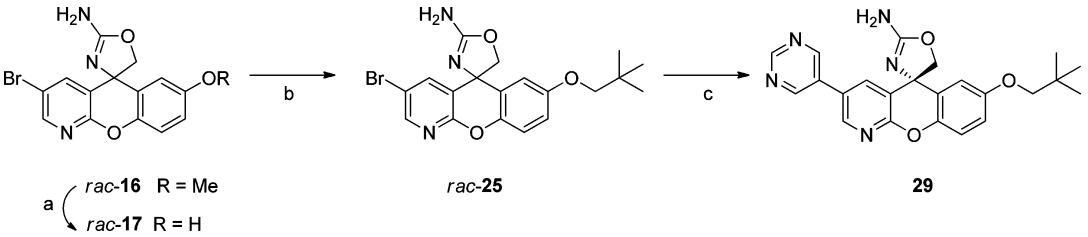

[a]Reagents: (a) BBr_3, DCM, 0 °C, 99%; (b) neopentyl iodide, Cs_2CO_3, DMF, 100 °C, 48%; (c) (i) 2-fluoro-3-pyridineboronic acid, $Pd(PPh_3)_4$, K_2CO_3, THF−water, sealed tube, 90 °C, (ii) chiral SFC, 24%.

Table 1. Evaluating Aza-substitution in the Xanthene Core

Cpd	Structure	BACE1 IC_{50} (nM) Enzyme[a]	BACE1 IC_{50} (nM) HEK[a,b]	hERG Ki (μM)	P_{app}[c]	Pgp Efflux[d] Human	Pgp Efflux[d] Rat	metabolic stability ((μL/min)/mg)[e] HLM	metabolic stability ((μL/min)/mg)[e] RLM
1	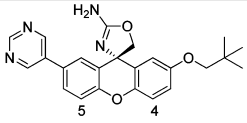	2.2 ± 1.1	25 ± 7.8	0.66	13	1.5	0.9	21	21
26	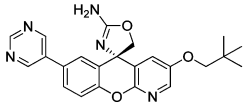	0.7 ± 0.04	4.4 ± 1.9	>10	16	2.3	3.2	47	22
27	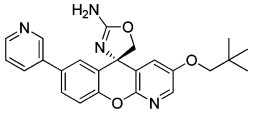	0.6 ± 0.2	3.8 ± 0.7	>10	11	1.8	1.0	55	136
28	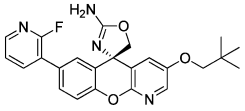	0.4 ± 0.08	2.6 ± 2.5	2.95	14	1.1	1.4	14	25
29	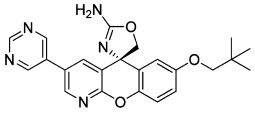	248 ± 55	1,350 ± 96	3.81	16	2.6	4.1	<14	<14

[a]Values represent the mean values of at least two experiments ± SD. [b]Human embryonic kidney cells. [c]Apparent permeability measured in parental LLC-PK1 cells. Values are an average of apical to basolateral (A to B) and basolateral to apical (B to A) velocities and are reported as 10^{-6} cm/s. [d]Efflux measured in LLC-PK1 cells transfected with either rat MDR1A/1B or human MDR1 and are reported as a ratio of (B to A)/(A to B). [e]Rat liver microsomal (RLM) and human liver microsomal (HLM) clearance. Compound concentration = 1 μM. Microsomal protein concentration = 250 μg/mL.

Selective Suzuki cross-coupling of the aryl iodide with 2-fluoro-3-pyridineboronic acid provided the penultimate bromide **13**, which was subjected to either a second Suzuki cross-coupling or a Sonogashira cross-coupling to generate the desired compounds in good overall yield.

Alternatively, other analogues (**33**−**37**) in Table 2 were prepared by initial coupling of the P2′ group followed by a final introduction of the 2-fluoro-3-pyridyl P3 group as described in Scheme 3. For these examples, phenol **14** and 2-chloropyridine **10** were converted to aminooxazoline **16** under the previously described conditions. Boron tribromide-mediated demethylation afforded bromophenol **17**, which served as a versatile intermediate for diverse Pd-catalyzed C,C and C,N cross-coupling reactions to install the P2′ group. Triflation of the phenols **18a**−**e** afforded triflates **19a**−**e**, which were subjected to a final Suzuki cross-coupling with 2-fluoro-3-pyridineboronic acid, yielding the desired compounds **33**−**37**.

The BACE1 inhibitor **30** was prepared via a separate route shown in Scheme 4. Xanthenone **21** was synthesized starting from bromophenol **3** and fluoropyridine **20** and was converted to bromophenol **22** via a two-step borylation-oxidation protocol. Formation of the 2-methoxy-2-methylpropoxy side chain of **24** was accomplished in four steps beginning with alkylation of the phenol with 3-bromo-2-methylpropene. The resulting alkene underwent iodo-etherification in the presence of NIS in methanol. Sequential treatment of the product with

dx.doi.org/10.1021/jm5012676 | J. Med. Chem. XXXX, XXX, XXX−XXX

Table 2. P2′ SAR of 4-Azaxanthenes

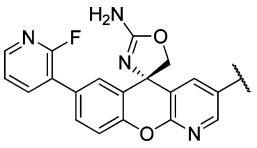

Cpd	R	BACE1 IC_{50} (nM) Enzyme[a]	BACE1 IC_{50} (nM) HEK[a,b]	hERG Ki (μM)	P_{app}[c]	Pgp Efflux[d] Human	Pgp Efflux[d] Rat	metabolic stability ((μL/min)/mg)[e] HLM	metabolic stability ((μL/min)/mg)[e] RLM
28	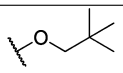	0.4 ± 0.08	2.6 ± 2.5	2.95	14	1.1	1.4	14	25
30	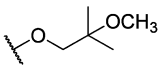	1.8 ± 0.06	6.6 ± 0.6	>10	16	12	12	67	53
31	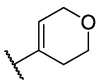	1.5 ± 0.06	5.2 ± 1.9	>10	20	29	16	26	36
32	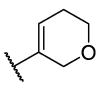	1.2 ± 0.05	5.2 ± 0.7	>10	11	4.1	6.1	18	16
33	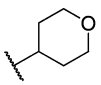	5.6 ± 0.02	19 ± 15	>10	15	21	18	14	14
34	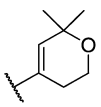	0.9 ± 0.02	6.6 ± 1.4	>10	17	1.6	2.2	14	54
35	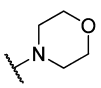	3.3 ± 0.3	16 ± 0.6	>10	10	35	36	14	14
36	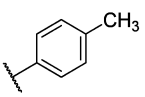	0.9 ± 0.07	14 ± 1.9	1.24	14	1.0	1.2	23	35
37	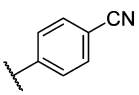	0.8 ± 0.06	8.2 ± 0.6	0.21	16	1.9	2.6	19	14
38	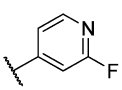	2.3 ± 0.02	15 ± 1.9	>10	15	6.6	8.4	14	14
39	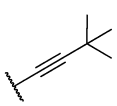	4.7 ± 0.1	4.5 ± 1.9	1.16	9.5	1	1	34	37
40	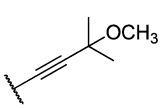	4.6 ± 0.03	2.8 ± 0.2	>10	12	2	2	261	54

[a]Values represent the mean values of at least two experiments ± SD. [b]Human embryonic kidney cells. [c]Apparent permeability measured in parental LLC-PK1 cells. Values are an average of apical to basolateral (A to B) and basolateral to apical (B to A) velocities and are reported as 10^{-6} cm/s. [d]Efflux measured in LLC-PK1 cells transfected with either rat MDR1A/1B or human MDR1 and are reported as a ratio of (B to A)/(A to B). [e]Rat liver microsomal (RLM) and human liver microsomal (HLM) clearance. Compound concentration = 1 μM. Microsomal protein concentration = 250 μg/mL.

MeMgCl and lithium triethylborohydride in a single pot afforded the alcohol **23**. Exposure of **23** to acid promoted elimination of the alcohol to form the exo-olefin, which was converted to the aminooxazoline **24**. A final Suzuki cross-coupling with 2-fluoro-3-pyridineboronic acid was followed by chiral separation to furnish compound **30**.

dx.doi.org/10.1021/jm5012676 | J. Med. Chem. XXXX, XXX, XXX–XXX

Table 3. Optimization of the P2′ Alkyne

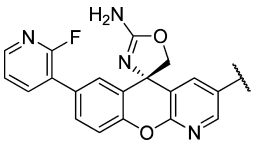

Cpd	R	BACE1 IC_{50} (nM) Enzyme[a]	BACE1 IC_{50} (nM) HEK[a,b]	hERG Ki (μM)	Pgp Efflux[d] P_{app}[c]	Pgp Efflux[d] Human	Pgp Efflux[d] Rat	metabolic stability ((μL/min)/mg)[e] HLM	metabolic stability ((μL/min)/mg)[e] RLM
40	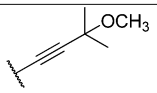	4.6 ± 0.03	2.8 ± 0.2	>10	12	2	2	261	54
41	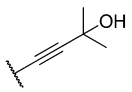	1.2 ± 0.3	5.6 ± 0.007	>10	11	>50	44	14	14
42 (AMG-8718)	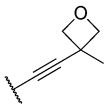	0.7 ± 0.3	4.4 ± 1.4	>10	19	5.8	9.2	33	16

[a]Values represent the mean values of at least two experiments ± SD. [b]Human embryonic kidney cells. [c]Apparent permeability measured in parental LLC-PK1 cells. Values are an average of apical to basolateral (A to B) and basolateral to apical (B to A) velocities and are reported as 10^{-6} cm/s. [d]Efflux measured in LLC-PK1 cells transfected with either rat MDR1A/1B or human MDR1 and are reported as a ratio of (B to A)/(A to B). [e]Rat liver microsomal (RLM) and human liver microsomal (HLM) clearance. Compound concentration = 1 μM. Microsomal protein concentration = 250 μg/mL.

The regioisomeric azaxanthene compound **29** (Table 1) was prepared as shown in Scheme 5. The racemic intermediate **16** (Scheme 1) was subjected to treatment with boron tribromide to give the corresponding phenol, which underwent a subsequent alkylation to form neopentyl ether **25**. Suzuki cross-coupling with 5-pyrimidyl boronic acid, followed by chiral separation, yielded the desired isomer **29**.

RESULTS AND DISCUSSION

Our previous work on aminooxazoline xanthene BACE1 inhibitors had demonstrated that incorporation of a fluorine atom in the xanthene core, especially at C(4), afforded a significant increase in enzymatic potency.[9] The enhanced potency was believed to arise from a favorable hydrogen-bonding interaction between the fluorine atom and NHTrp76 of the protein, and we hypothesized that a nitrogen atom at the 4-position of the xanthene could similarly engage Trp76. Furthermore, employing a nitrogen atom to exploit this interaction with the protein could not only potentially boost potency against BACE1 but at the same time reduce hERG binding affinity as a result of the increase in PSA.[14] While there was a possibility that the additional PSA could result in increased transporter-mediated efflux,[15] the consequential decreased exposure in the CNS could potentially be offset by increases in BACE1 potency, enabling the discovery of BACE1 inhibitors with good in vivo efficacy and improved cardiovascular safety margins.

We began our investigation by preparing **26**, the 4-aza analogue of one of our initial leads, **1**. As shown in Table 1, the 4-azaxanthene core did indeed afford both greater enzymatic and functional potency than the all-carbon analogue **1**. As expected, the higher PSA led to a hERG binding K_i >10 μM in addition to a slight increase in Pgp-mediated efflux ratios to >2, indicating that compound **26** is a Pgp-substrate. Reducing the overall PSA of the molecule by changing the P3 group from a 5-pyrimidyl to a 3-pyridyl ring (**27**), isomeric with compound **1**, returned the favorable efflux properties of **1** while maintaining low hERG activity. Replacement of the P3 group with the 2-fluoro-3-pyridyl ring (**28**) generated a compound with excellent BACE1 potency in our enzymatic and functional assays, low efflux ratios, and moderate hERG binding. We also examined incorporation of a nitrogen atom at the 5-position of the xanthene. Compound **29** showed dramatically reduced BACE1 potency in the enzymatic and functional assays, suggesting an unfavorable interaction of this atom with the protein. Interestingly, incorporation of a nitrogen atom at the 4-position led to decreases in microsomal stability when coupled with either a 5-pyrimidine (**26**) or a 3-pyridyl group (**27**) in P3, however, the 2-fluoro-3-pyridyl analogue (**28**) maintained the low metabolism observed with all-carbon analogue **1**.

As mentioned before, compound **28** demonstrated improved BACE1 functional potency and decreased hERG activity, relative to **1**, while maintaining the high permeability, low Pgp efflux, and good microsomal stability—properties consistent with good distribution into the CNS. In an effort to further reduce hERG activity within this series, additional P2′ side chains were explored. As shown in Table 2, a number of groups which had previously been identified as beneficial for BACE1 potency[9] were incorporated into the P2′ side chain of the 4-azaxanthene aminooxazolines. Addition of a methoxy group to the neopentyloxy P2′ side chain (**30**) resulted in a slight decrease of BACE1 enzymatic and functional potencies. Inhibitors containing a dihydropyran P2′ group (**31**, **32**, and **34**) were all approximately 2-fold less potent than **28**, and the fully saturated tetrahydropyran **33** was approximately 8-fold less potent in the functional assay. Similarly, the *N*-morpholino

dx.doi.org/10.1021/jm5012676 | J. Med. Chem. XXXX, XXX, XXX−XXX

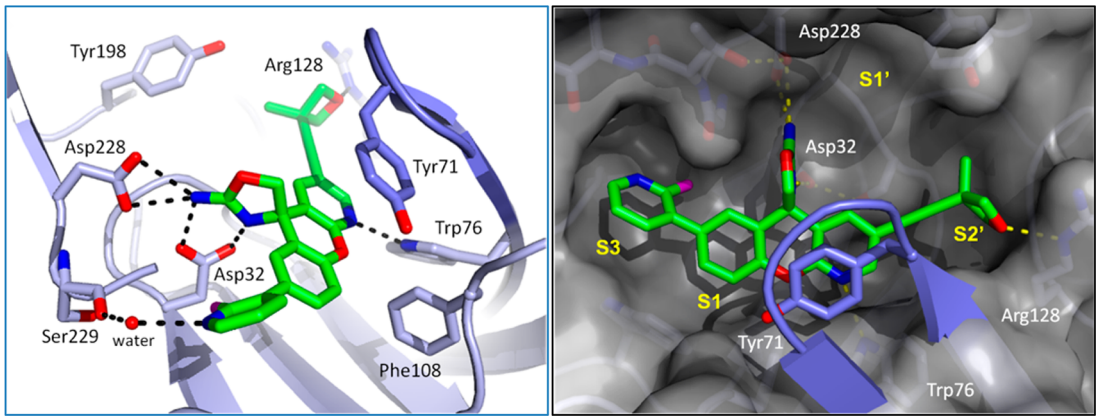

Figure 2. Co-crystal structure of **42** with BACE1. (a) Interactions of **42** with the catalytic aspartic acids, Ser229, and Trp76 of BACE1. (b) Interaction of the P2′ oxetane unit with Arg128 in S2′.

Table 4. Reduction of CSF Aβ_{40} in Wild-Type Sprague–Dawley Rats

compd[a]	CSF Aβ_{40} reduction[b] (%)	brain Aβ_{40} reduction[b] (%)	[plasma]$_{total}$ (μM)[c]	[plasma]$_{unbound}$ (μM)[c]	[CSF] (μM)[d]	[CSF]/cell IC$_{50}$
34	53	16	1.01	0.045	0.005	0.75
42	69	48	4.43	0.059	0.017	3.9

[a]Compounds were dosed orally at 10 mg/kg as a solution (2% HMPC, 1% Tween80) to male rats. n = 5 animals per group. [b]CSF and brain Aβ_{40} measured at t = 4 h. [c]Plasma drug concentration measured at t = 4 h. [d]CSF drug concentration measured at t = 4 h.

substituent in compound **35** resulted in reduced BACE1 activity in both the enzymatic and functional assays. While compounds with aryl groups in P2′ (**36**–**38**) maintained good potency in the BACE1 enzymatic assay, they were consistently less potent (approximately 3–6-fold) in the functional assay. Finally, alkynes **39** and **40** demonstrated no enzyme-to-cell shift and consequently produced low nanomolar inhibitors in the functional cellular assay.

Most compounds with a polar heteroatom incorporated in the P2′ side chain showed significantly decreased hERG binding affinity (K_i > 10 μM), albeit in some cases at the expense of increased human and rat Pgp recognition. For example, Pgp efflux ratios for ethereal compounds **30**, **31**, **33**, and **35** were >10. Shielding of the ethereal oxygen with methyl substitution, as in dihydropyran **34**, resulted in a favorable combination of low hERG binding affinity and low Pgp efflux ratios. The dihydropyran isomer **32** showed modest efflux when compared with close structural analogues **31** and **33**. Tolyl-substituted inhibitor **36** and aryl nitrile **37** both maintained significant hERG binding activity, while fluoropyridine **38** had hERG K_i > 10 μM. Compound **37** showed reduced Pgp efflux activity compared to compound **38**. Incorporation of a methoxy group into the *t*-butylacetylene unit of compound **39** yielded a compound with excellent BACE1 potency, low activity in hERG binding assay, and low efflux ratios (**40**).

Most compounds we examined were stable in human and rat liver microsomes, with the exception of compound **40**. Given the attractive overall profile of **40**, we sought to further understand its high intrinsic clearance with the aim of generating a more metabolically stable analogue. Metabolite identification studies on a related analogue with the same P2′ side chain (data not shown), suggested that the methoxy ether of **40** may undergo oxidative demethylation to form alkynol **41** (Table 3). In support of this hypothesis, alkynol **41** was independently synthesized and found to be stable in human and rat liver microsomes. Although this compound also showed good BACE1 potency and low activity in the hERG binding assay, it was subject to extremely high Pgp efflux (efflux ratio = >50 and 44 for human and rat, respectively), likely as a result of the additional hydrogen bond donor of the free alcohol. To combine the low intrinsic clearance of alkynol **41** with the low efflux ratios of methyl ether **40**, an inhibitor featuring a 3-methyl-3-oxetane ethynyl group in P2′ (**42**) was targeted. The oxetane group was predicted to be more stable toward oxidative dealkylation, and it was expected to be less likely a Pgp recognition element.[15] In fact, compound **42** (AMG-8718) exhibited good stability in human and rat liver microsomes and only modest Pgp efflux ratios. Importantly, this compound demonstrated high BACE1 potency, low activity in the hERG binding assay, and excellent permeability.

An X-ray cocrystal structure of compound **42** with BACE1 is shown in Figure 2.[16] As observed in previous cocrystallized BACE1 inhibitors, the aminooxazoline unit engages in hydrogen-bonding interactions with the catalytic aspartic acid residues of the enzyme, and the nitrogen atom of the 2-pyridyl-3-fluoro group interacts with Ser229 via a bridging water molecule in the S3 pocket. As anticipated, the nitrogen atom in the xanthene ring system engages Trp76 in a hydrogen-bonding interaction, likely resulting in the enhanced potency observed for 4-azaxanthenes relative to their all-carbon analogues. An additional hydrogen-bonding interaction in S2′ was observed between the oxetane oxygen and Arg128.

A potential concern with compound **42** was the possibility of CYP inactivation as a result of oxidation of the alkynyl group to form reactive metabolites,[17] however, no time-dependent inhibition of CYP activity was detected when **42** was examined in IC$_{50}$ shift experiments (30 min incubation).[18] Additionally, given the potentially reactive nature of the 2-fluoropyridine and oxetane functional groups, **42** was incubated in buffered solutions in the presence of glutathione (GSH), as well as with hepatocytes, and no incorporation of GSH was observed under these conditions.

dx.doi.org/10.1021/jm5012676 | J. Med. Chem. XXXX, XXX, XXX–XXX

BACE inhibitors **34** and **42** possessed a good overall balance of properties (BACE1 functional potency, permeability, intrinsic stability, and Pgp efflux ratios) and were therefore evaluated in vivo for their ability reduce the concentration of CNS Aβ in a rat pharmacodynamic model. Male Sprague–Dawley rats were dosed with compounds **34** or **42** (10 mg/kg) by oral gavage, where after 4 h plasma and CSF drug levels were determined along with Aβ_{40} concentrations in the CSF and brain.[19] As shown in Table 4, both compounds **34** and **42** significantly decreased Aβ_{40} levels in the CSF at the 4 h time point (53% and 69%, respectively), however, only **42** produced a robust response in the brain (48% reduction of Aβ_{40} levels for **42** vs 16% for **34**). The reason for this disparity is potentially due to a difference in exposure multiples for the two compounds in the brain. Although both compounds achieved similar unbound concentrations in plasma at the 4 h time point, **42** achieved an approximately 5-fold higher exposure than **34** in the CSF compartment, which may reflect a higher unbound concentration in the brain. However, it is possible that CSF concentrations may be inflated relative to unbound brain concentrations as a result of active blood-to-CSF transport by Pgp.[20]

On the basis of the more significant pharmacodynamic response observed with **42**, the pharmacokinetic behavior of this compound in rat, dog, and cynomolgus monkey was evaluated. Consistent with its stability in liver microsomes, **42** showed moderate total clearance, moderate V_{dss}, and half-lives of ca. 5–8 h across all three species (Table 5). The clearance in cynomolgus monkey was roughly double that of rat and dog, an observation which can be partially accounted for by the larger unbound fraction in plasma for monkey relative to rat and dog. When dosed orally, bioavailability was high (70–101%) across all three species, and the compound was rapidly absorbed as indicated by t_{max} of 1–2 h.

Table 5. Pharmacokinetic Profiles and Plasma Protein Binding of 42

	iv[a]			po[b]			
species[a]	Cl (L/h/kg)	V_{dss} (L/kg)	$t_{1/2}$ (h)	C_{max} (μM)	t_{max} (h)	% F	plasma protein binding (F_u)
rat	0.33	1.1	4.8	3.8	1.7	70	0.013
beagle dog	0.26	1.6	5.2	8.1	1.0	96	0.038
monkey	0.61	2.2	7.7	6.1	1.7	101	0.054

[a]2 mg/kg iv dose as a solution in DMSO (rat), 1% Tween80/2% HMPC/97% water at pH = 4 (dog), or 25% HBC/75% water at pH = 4 (cynomolgus monkey). [b]5 mg/kg oral dose as a solution in 1% Tween80/2% HMPC/97% water at pH = 2.

Because **42** achieved good exposure in rats following oral administration, a dose–response relationship of this compound on CNS Aβ levels in the rat pharmacodynamic model was determined. As shown in Figure 3, **42** demonstrated dose-dependent decreases in both CSF and brain Aβ levels at 4 h time points. The reduction in Aβ levels tended to be more significant in the CSF than in the brain, although the values were generally within 2-fold and ≥70% Aβ reduction was achieved in both the CSF and brain at a dose of 30 mg/kg. The effective unbound plasma drug concentration corresponding to 50% Aβ reduction ($EC_{50,unbound}$) at the 4 h time point was calculated to be 18 and 67 nM for CSF and brain, respectively. The temporal effects of **42** on CNS Aβ levels were examined in a time-course pharmacodynamic study in rat at 30 mg/kg. As shown in Figure 3, **42** demonstrated robust and sustained reduction of Aβ levels in both the CSF and brain for over 8 h. The lowest concentrations of Aβ in both compartments were observed between 4 and 5 h, and the concentrations of Aβ returned to predosing levels within 16–20 h. The changes in brain Aβ concentration tended to precede those in the CSF by a small margin. Using an indirect response PK/PD model,[21] which accounts for the rate of Aβ formation and clearance in the rat CNS, the in vivo plasma $IC_{50,unbound}$ of **42** was determined to be 62 nM. The difference between the in vivo $IC_{50,unbound}$ and the IC_{50} of **42** in the BACE1 functional assay (4.4 nM) is likely due, in part, to reduced exposure in the brain as a result of Pgp efflux.

The effects of **42** in an anesthetized dog cardiovascular safety model were studied. The compound was administered intravenously as a series of three 30 min infusions at doses of 2.5, 8, and 16 mg/kg to two chloralose-anesthetized dogs. The unbound plasma concentrations were assessed at the end of each infusion and determined (average) to be 0.298, 1.70, and 3.62 μM, respectively. No significant effects on the QTc interval were observed at these doses. The unbound plasma concentration at the high dose was 201-fold over the plasma $EC_{50,unbound}$ for CSF Aβ reduction in rats and 58-fold over the in vivo $IC_{50,unbound}$ as determined by the indirect response model. The margins observed in this study represent a significant improvement over compounds like **1** and **2**.

Our strategy of installing a nitrogen atom at the 4-position of the xanthene to engage Trp76 resulted in the discovery of BACE1 inhibitors with increased BACE1 potency and reduced hERG binding affinity. An optimized compound from this series, **42**, showed a 5-fold improvement in BACE1 functional potency compared with **1**, an earlier lead (Figure 4, Table 6). Although these compounds have similar total PSA, **42** is more polar (log P = 2.53 for **42** vs log P = 5.20 for **1**), which may account for the significantly lower activity of this compound in the hERG binding assay.[14] The impact of increased Pgp efflux for **42** observed in the in vitro assays was mitigated by the high functional potency and permeability of this compound, resulting in robust reductions in CNS Aβ in the rat pharmacodynamic model. As a result of the balance of BACE1 potency, hERG binding affinity, and Pgp recognition for compound **42**, significantly higher safety margins for elongation of the QTc interval in the dog cardiovascular model relative the EC_{50} and IC_{50} measured in the rat pharmacodynamic model were achieved.

Finally, compounds **1** and **42** were tested against a panel of other aspartyl proteases. Both compounds demonstrated limited selectivity for BACE1 over homologue BACE2, and the high selectivity for BACE1 over both renin and pepsin observed with **1** was preserved with **42**. Although **1** showed only modest selectivity for BACE1 against cathepsins D and E (478× and 139×, respectively), **42** was very selective (3285× and 1429×, respectively), a result of both increased BACE1 potency and lower cathepsin activity for this compound.

CONCLUSION

A novel series of potent BACE1 inhibitors was discovered by incorporating a nitrogen atom into the 4-position of the aminooxazoline xanthene scaffold. The nitrogen atom led to improved BACE1 potency, reduced hERG binding affinity, and elevated Pgp efflux ratios. Optimization of the P3 group and exploration of the P2′ group resulted in several compounds

dx.doi.org/10.1021/jm5012676 | J. Med. Chem. XXXX, XXX, XXX–XXX

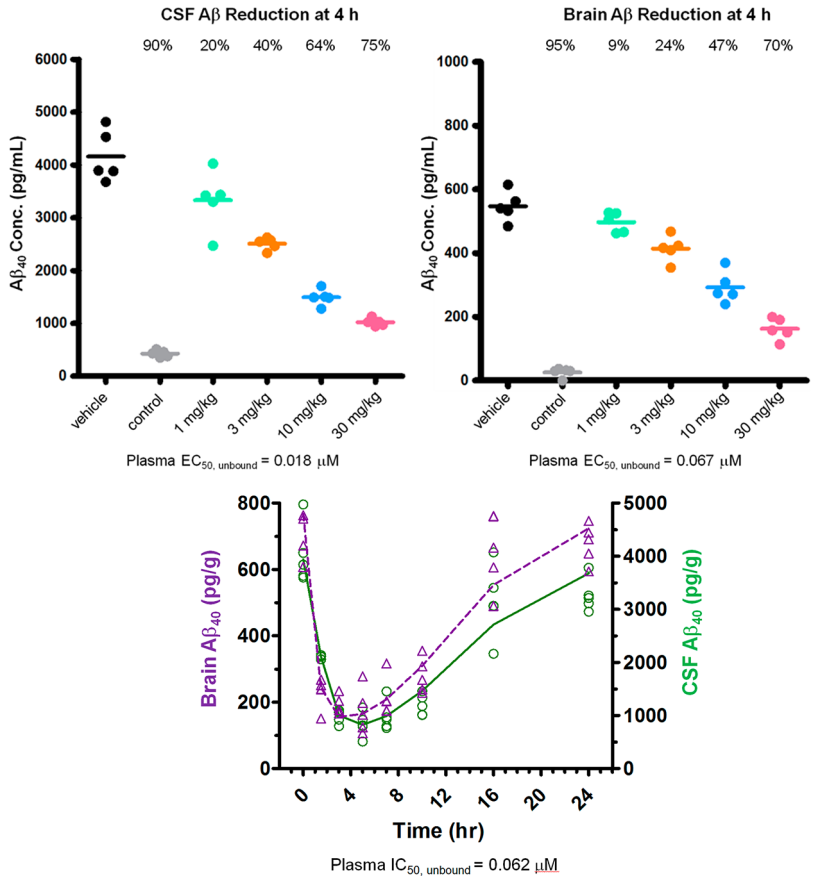

Figure 3. Pharmacodynamic effect of **42** on CNS Aβ in Sprague–Dawley rats. (a) CSF Aβ reduction at 4 h. (b) Brain Aβ reduction at 4 h. (c) Time-course study at 30 mg/kg.

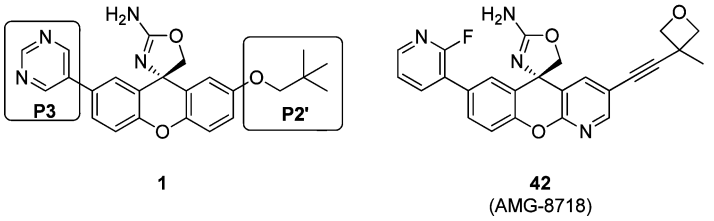

	1	42
BACE1 IC_{50} (nM):	2.2	0.7
BACE Cellular IC_{50} (nM):	25	4.4
Papp ($x10^{-6}$ cm/s):	13	19
Human / Rat Pgp ER:	1.5 / 0.9	5.8 / 9.2
hERG Ki (μM):	0.66	>10
logP:	5.20	2.53
PSA:	92	92

Figure 4. Comparison of BACE Inhibitors **1** and **42**.

Table 6. Aspartyl Protease Selectivity of 1 and 42

	protease IC_{50} (μM)/selectivity					
	BACE1	BACE2	renin	pepsin	cathepsin D	cathepsin E
1	0.0023	0.015 (7×)	>3 (1300×)	9.5 (4130×)	1.1 (478×)	0.32 (139×)
42	0.0007	0.005 (7×)	>1 (1429×)	>1 (1429×)	2.3 (3285×)	>1 (1429×)

with improved in vitro profiles. An oxetane-containing P2′ group was designed to balance Pgp efflux and microsomal turnover, and this effort culminated in the identification of inhibitor **42**. Although this compound was a moderate Pgp substrate, it led to robust and sustained reductions of CSF and brain Aβ in a rat pharmacodynamic model. In accordance with low hERG binding affinity, **42** did not result in elongation of the QTc interval at plasma concentrations exceeding 108-fold and 31-fold over the plasma $EC_{50,unbound}$ for CSF Aβ reduction and the vivo plasma $IC_{50,unbound}$, respectively. Further studies detailing pharmacodynamic and toxicology studies of this compound will be reported in due course.

EXPERIMENTAL SECTION

BACE1 Enzymatic Assay. BACE1 enzymatic activity was determined by the enhancement of fluorescence intensity upon enzymatic cleavage of the fluorescence resonance energy transfer substrate according to a previously published procedure.[6p]

Cell-Based Assay. BACE 1 cellular activity was determined in human embryonic kidney cells (HEK293) stably expressing APP_{SW}. After incubation overnight with the test compounds, the conditioned

dx.doi.org/10.1021/jm5012676 | J. Med. Chem. XXXX, XXX, XXX–XXX

media was collected and the Aβ40 levels were determined using a sandwich ELISA as described previously.[6p]

Permeability Assay. Permeability and efflux ratios were determined in the wild-type cell line LLC-PK1 (porcine renal epithelial cells, WT-LLC-PK1) transfected with human *MDR1* gene (hMDR1-LLC-PK1) and rat *mdr1a* gene (rMdr1a-LLC-PK1) as described previously.[6p]

Microsomal Stability Assay. Compounds (1 μM) were incubated with liver microsomes from human and rat for 30 min at 37 °C, and the samples were analyzed according to published procedure.[8]

hERG Binding Assay. A stable HEK293 cell line expressing the hERG channel was established in house. Compounds were tested in the [^{3}H]-dofetilide binding assay with cell membranes prepared from this cell line by using the method of Finlayson with some modifications.[22] Briefly, filtration assays were carried out in 194 μL of binding buffer (10 mM HEPES, pH 7.4, 60 mM KCl, 71.5 mM NaCl, 1 mM $CaCl_2$, 2 mM $MgCl_2$) with 10 μg/well membrane (based on membrane protein) and [^{3}H]-dofetilide (8 nM), 6 μL of compound dissolved in 100% DMSO. Nonspecific binding was determined by using 10 μM cold dofetilide (~1000-fold molar excess over hot ligand). The entire assay was conducted in 96-well Whatman Unifilter plates at room temperature for 90 min. The binding assay was terminated by washing the plates four times on a Millipore vacuum filtration manifold with 100 μL/well of ice-cold wash buffer (10 mM HEPES, pH 7.4, 131.5 mM NaCl, 1 mM $CaCl_2$, 2 mM $MgCl_2$). The bound radioisotope was quantified using a Packard TopCount NTS liquid scintillation counter with scintillation fluid.

Pharmacodynamic Assay. Male Sprague–Dawley rats (175–200 g) were administered compound by oral gavage at the appropriate dose. Samples of plasma, CSF, and brain were analyzed according to previously reported procedures.[6p]

Chemistry. Unless otherwise noted, all materials were obtained from commercial suppliers and used without further purification. Anhydrous solvents were obtained from Aldrich or EM Science and used directly. All reactions involving air- or moisture-sensitive reagents were performed under a nitrogen or argon atmosphere. All microwave assisted reactions were conducted with a Smith synthesizer from Personal Chemistry, Uppsala, Sweden. Silica gel chromatography was performed using either glass columns packed with silica gel (230–400 mesh, EMD Chemicals, Gibbstown, NJ) or prepacked silica gel cartridges (Biotage or ISCO). ^{1}H NMR spectra were recorded on a Bruker AV-400 (400 MHz) spectrometer at ambient temperature or on a Varian 400 MHz spectrometer. Chemical shifts are reported in parts per million (ppm, δ units) downfield from tetramethylsilane. Data are reported as follows: chemical shift, multiplicity (s = singlet, d = doublet, t = triplet, q = quartet, br = broad, m = multiplet), coupling constants, and number of protons. Purity for final compounds was greater than 95% unless otherwise noted and was measured using Agilent 1100 series high performance liquid chromatography (HPLC) systems with UV detection at 254 nm (system A, Agilent Zorbax Eclipse XDB-C8 4.6 mm × 150 mm, 5 μm, 5–100% CH_3CN in H_2O with 0.1% TFA for 15 min at 1.5 mL/min; system B, Waters Xterra 4.6 mm × 150 mm, 3.5 μm, 5–95% CH_3CN in H_2O with 0.1% TFA for 15 min at 1.0 mL/min). Exact mass confirmation was performed on an Agilent 1100 series high performance liquid chromatography (HPLC) system (Santa Clara, CA, U.S.) by flow injection analysis, eluting with a binary solvent system A and B (A, water with 0.1% FA; B, ACN with 0.1% FA) under isocratic conditions (50% A/50% B) at 0.2 mL/min with MS detection by an Agilent G1969A time-of-flight (TOF) mass spectrometer (Santa Clara, CA, U.S.).

*7-Bromo-3-methoxy-5H-chromeno[2,3-b]pyridin-5-one (**5**).* Step 1: 2-(4-Bromophenoxy)-5-methoxynicotinic acid. To a slurry of sodium hydride (60% dispersion) (5.14 g, 129 mmol) in DMF (106 mL, 58.4 mmol) at 0 °C was added 4-bromophenol (11.12 g, 64.3 mmol), resulting in the evolution of hydrogen gas. The mixture was stirred at 0 °C for 2 min then for an additional 5 min at room temperature. 2-Fluoro-5-methoxynicotinic acid (10.0 g, 58.4 mmol) was added portionwise over 1 min. The resulting slurry was heated to 130 °C for 20 h, then heated to 140 °C for another 3 h. The reaction mixture was cooled to room temperature and poured onto 500 g of ice. Acetic acid (16.73 mL, 292 mmol) was added, and the resulting taffy was stirred vigorously for 2 h, resulting in the formation of a fine off-white precipitate. The slurry was filtered, and the collected solid was washed with methanol, washed ether, and then dried to give 2-(4-bromophenoxy)-5-methoxynicotinic acid (10.5 g, 55% yield) as an off-white solid. ^{1}H NMR (400 MHz, DMSO-d_6) δ = 13.42 (br s, 1 H), 8.06 (d, *J* = 3.1 Hz, 1 H), 7.81 (d, *J* = 3.1 Hz, 1 H), 7.60–7.50 (m, 2 H), 7.01–6.94 (m, 2 H), 3.85 (s, 3 H). MS *m*/*z* = 324.0 [M + H]$^+$. Calcd for $C_{13}H_{11}BrNO_4$: 324.0.

Step 2: 7-Bromo-3-methoxy-5*H*-chromeno[2,3-*b*]pyridin-5-one. 2-(4-Bromophenoxy)-5-methoxynicotinic acid (8.00 g, 24.68 mmol) was added to a round-bottom flask containing polyphosphoric acid (115% H_3PO_4) (75 g, 24.68 mmol) that had been warmed to 140 °C. The resulting mixture was stirred at this temperature for 3.5 h. The reaction mixture was allowed to cool to 100 °C and then poured into 500 mL of ice–water. The resulting thick taffy was stirred vigorously, leading to the formation of a fine white precipitate. Stirring was continued for 1 h, at which point the mixture was filtered. The collected solid was washed with MeOH (2 × 100 mL), washed with diethyl ether (3 × 100 mL), and dried to give 7-bromo-3-methoxy-5*H*-chromeno[2,3-*b*]pyridin-5-one (7.05 g, 93% yield) as a fine-white solid. ^{1}H NMR (400 MHz, DMSO-d_6) δ = 8.71 (d, *J* = 3.3 Hz, 1 H), 8.35 (d, *J* = 2.4 Hz, 1 H), 8.20–8.12 (m, 2 H), 7.86 (d, *J* = 8.9 Hz, 1 H), 4.07 (s, 3 H).

*(S)-7-Bromo-3-methoxy-5′H-spiro[chromeno[2,3-b]pyridine-5,4′-oxazol]-2′-amine (**6**).* To a slurry of 7-bromo-3-methoxy-5*H*-chromeno[2,3-*b*]pyridin-5-one (23 g, 75 mmol) in THF (751 mL, 75 mmol) at −40 °C was added methylmagnesium chloride (3 M solution in THF, 88 mL, 263 mmol) over 2 min, such that the temperature did not rise above −35 °C. The resulting red slurry was maintained at −30 °C. After 1 h, the reaction mixture was quenched by the addition of EtOAc (50 mL). The solution was then carefully quenched with 800 mL of a 50% aq ammonium chloride solution. The mixture was poured into a separatory funnel containing ethyl acetate (100 mL). The layers were separated, and the organic layer was washed with brine, dried over sodium sulfate, filtered, and concentrated. The aqueous layer was extracted with ethyl acetate (3 × 500 mL). The combined organic layers were washed with water and then brine, dried over sodium sulfate, filtered, and combined with the first lot of residue. This organic solution was washed with brined, dried over sodium sulfate, fitlered, and concentrated to provide a yellow solid which was used directly in the next reaction.

Step 2: To a solution of 7-bromo-3-methoxy-5-methyl-5*H*-chromeno[2,3-*b*]pyridin-5-ol (23.5 g, 72.9 mmol, from step 1) in THF (729 mL, 72.9 mmol) was added HCl (1 M in ether) (0.729 mL, 0.729 mmol). After heating at 45 °C for 10 min, more HCl (1 M in ether) (0.729 mL, 0.729 mmol) was added. The reaction was heated at 45 °C for a total of 30 min, at which point TLC indicated complete conversion to olefin. This light-yellow solution was cooled to −25 °C and added to the slurry generated below.

To a solution of iodine (20.37 g, 80 mmol) and THF (400 mL) at −15 °C was added silver cyanate (32.8 g, 219 mmol). The resulting slurry was maintained at −40 °C for 25 min, and then the olefin solution (generated above) was added via cannula over 15 min, maintaining the temperature below −35 °C. The derived slurry was maintained at −30 °C for 1 h and then was filtered through a pad of Celite, washing well with 200 mL of THF. The derived brown solution was cooled to −20 °C and treated with ammonia (2.0 M in 2-propanol, 219 mL, 438 mmol). The resulting solution was allowed to slowly warm to room temperature overnight. To the reaction was added 10% aq sodium thiosulfate solution (700 mL), and the resulting light-orange solution was stirred for 10 min before being poured into a separatory funnel containing EtOAc (250 mL). The layers were separated, and the organic layer was washed with brine and concentrated in vacuo to provide an orange mixture still containing a considerable amount of water. This mixture was combined with the organic extracts obtained below.The aqueous layer was extracted with ethyl acetate (2 × 500 mL). These organics were combined with the organics obtained and poured into a separatory funnel. The layers were separated, and the aqueous layer was extracted with ethyl acetate (2 × 100 mL). The combined organic layers were washed with brine, dried

dx.doi.org/10.1021/jm5012676 | J. Med. Chem. XXXX, XXX, XXX–XXX

over sodium sulfate, filtered, and concentrated in vacuo to provide 25 g of racemic 7-bromo-3-methoxy-5′*H*-spiro[chromeno[2,3-*b*]pyridine-5,4′-oxazol]-2′-amine as a brown solid. This material was dissolved in DCM (200 mL) and MeOH (200 mL). The solution was purified by chromatography, using 6 mL injections on a 5 μm, 5 cm × 15 cm Chiralpak AD column with 50% MeOH/0.2% diethylamine/50% CO_2 at a flow rate of 250 mL/min to afford peak 1, (*R*)-7-bromo-3-methoxy-5′*H*-spiro[chromeno[2,3-*b*]pyridine-5,4′-oxazol]-2′-amine (8.235 g, 22.74 mmol, 31.2% yield), and peak 2, (*S*)-7-bromo-3-methoxy-5′*H*-spiro[chromeno[2,3-*b*]pyridine-5,4′-oxazol]-2′-amine (7.53 g, 20.79 mmol, 28.5% yield). ^{1}H NMR (400 MHz, DMSO-d_6) δ = 8.30−8.22 (m, 1 H), 7.66 (d, *J* = 2.2 Hz, 1 H), 7.17 (d, *J* = 9.0 Hz, 1 H), 6.96 (dd, *J* = 3.0, 8.9 Hz, 1 H), 6.83 (d, *J* = 3.0 Hz, 1 H), 6.55 (br s, 2 H), 5.50 (s, 1 H), 4.29−4.10 (m, 2 H), 3.76 (s, 3 H). MS *m*/*z* = 362.0 [M + H]$^+$. Calcd for $C_{15}H_{13}BrN_3O$: 362.0.

*(S)-2′-Amino-7-bromo-5′H-spiro[chromeno[2,3-b]pyridine-5,4′-oxazol]-3-ol (**7**).* To a solution of (*S*)-7-bromo-3-methoxy-5′*H*-spiro[chromeno[2,3-*b*]pyridine-5,4′-oxazol]-2′-amine (**6**) (6.0 g, 16.57 mmol) in DCM (166 mL) at 0 °C was added boron tribromide (9.40 mL, 99 mmol). This led to the immediate formation of a light-orange precipitate. The resulting slurry was removed from the ice bath and allowed to stir at room temperature for 12 h. The mixture was cooled to −20 °C and treated with methanol (6.70 mL, 166 mmol), followed immediately by saturated aq sodium bicarbonate (1 L). DCM (500 mL) was added, and the mixture was warmed to room temperature. The layers were separated, and the aqueous layer was extracted with methylene chloride (500 mL). The combined organic layers were washed with brine and dried over sodium sulfate. The aqueous layer was then extracted with ethyl acetate (2 × 500 mL). The combined organics were washed with brine, dried over sodium sulfate, and combined with the organic solution obtained above. The aqueous layer was then stirred overnight with 500 mL of ethyl acetate. The organic layer was removed, washed with brine, dried over sodium sulfate, and filtered. This solution was combined with the organic layers above and concentrated in vacuo to provide an orange solid. This solid was taken up in 10 mL of DCM and purified by silica gel chromatography (0−10% MeOH/DCM with 0.1% ammonium hydroxide) to provide (*S*)-2′-amino-7-bromo-5′*H*-spiro[chromeno-[2,3-*b*]pyridine-5,4′-oxazol]-3-ol (2.95 g, 8.47 mmol, 51.1% yield) as a light-orange solid. ^{1}H NMR (400 MHz, DMSO-d_6) δ = 9.88 (br s, 1 H), 7.81 (d, *J* = 2.7 Hz, 1 H), 7.59−7.44 (m, 2 H), 7.28−7.12 (m, 2 H), 4.31 (br s, 2 H), 4.06 (q, *J* = 5.2 Hz, 1 H), 3.18 (s, 1 H), 3.16 (s, 1 H).

*(S)-7-Bromo-3-(neopentyloxy)-5′H-spiro[chromeno[2,3-b]-pyridine-5,4′-oxazol]-2′-amine (**8**).* To a solution of (*S*)-2′-amino-7-bromo-5′*H*-spiro[chromeno[2,3-*b*]pyridine-5,4′-oxazol]-3-ol (0.900 g, 2.59 mmol) in *N*,*N*-dimethylformamide (10.34 mL, 2.59 mmol) at rt was added cesium carbonate (2.106 g, 6.46 mmol). The mixture was stirred for a 1 min, and then 1-iodo-2,2-dimethylpropane (0.514 mL, 3.88 mmol) was added. The mixture was heated to 100 °C for 3 h. After cooling to room temperature, the reaction mixture was diluted with water (250 mL) and poured into a separatory funnel containing ethyl acetate (250 mL). The layers were separated, and the aqueous layer was extracted with ethyl acetate (3 × 200 mL). The combined organic layers were washed with water and then brine, dried over sodium sulfate, filtered, and concentrated. The aq layer was then extracted with DCM (4 × 150 mL). The combined organics were washed with brine, dried over sodium sulfate, filtered, and concentrated. The two residues were combined, and the combined residue was purified by chromatography on silica gel (0−10% MeOH/DCM 0.1% ammonium hydroxide). The resulting material was purified again by chromatography on silica gel (0−100% EtOAc/DCM) to provide (*S*)-7-bromo-3-(neopentyloxy)-5′*H*-spiro-[chromeno[2,3-*b*]pyridine-5,4′-oxazol]-2′-amine (680 mg, 1.626 mmol, 62.9% yield) as an orange solid. MS *m*/*z* = 418.0 [M + H]$^+$. Calcd for $C_{19}H_{21}BrN_3O_3$: 418.0.

*3-Bromo-7-iodo-5H-chromeno[2,3-b]pyridin-5-one (**11**).* Step 1: 5-Bromo-2-(4-iodophenoxy)nicotinic acid, a round-bottom flask under N_2(g) was charged with sodium hydride (22.40 g, 560 mmol) and DMF (540 mL). The slurry was cooled to 0 °C and carefully treated with 4-iodophenol (58.6 g, 266 mmol) portionwise, resulting in bubbling. After the bubbling had subsided, 5-bromo-2-chloronicotinic acid (60.2 g, 255 mmol) was then added to slurry portionwise and the resulting mixture was heated to 115 °C overnight. The mixture was cooled to room temperature then diluted with water (240 mL). Acetic acid (ca. 60 mL) was added until the mixture achieved pH of 4−5. Water (1260 mL) was added via addition funnel, and the resulting mixture was cooled in an ice-bath for 1.5 h. The mixture was filtered, and the collected solid was washed with water and dried on the filter overnight to give 5-bromo-2-(4-iodophenoxy)nicotinic acid (80.9 g, 76%) as a light-brown solid. ^{1}H NMR (400 MHz, DMSO-d_6) δ = 13.56 (br s, 1 H), 8.40 (dd, *J* = 2.6, 13.4 Hz, 2 H), 7.82−7.60 (m, 2 H), 7.05−6.80 (m, 2 H). MS *m*/*z* = 420.0 [M + H]$^+$. Calcd for $C_{12}H_8BrINO_3$: 419.9.

Step 2: 3-Bromo-7-iodo-5*H*-chromeno[2,3-*b*]pyridin-5-one, 5-bromo-2-(4-iodophenoxy)nicotinic acid (80.9 g, 193 mmol) was added portionwise to a round-bottom flask containing polyphosphoric acid at 110 °C. When the addition was complete, the mixture was stirred at 110 °C overnight and then at 140 °C for 1.5 h. The mixture was cooled to 35 °C and then added slowly to ice-cold water (1.2 L). The resulting slurry was stirred for 1 h at room temperature, and then the solid was filtered. The collected solid was washed with water (2×), washed with 2-PrOH, and dried under vacuum to give 3-bromo-7-iodo-5*H*-chromeno[2,3-*b*]pyridin-5-one (65.9 g, 85%) as a white solid. ^{1}H NMR (400 MHz, DMSO-d_6) δ = 8.95 (d, *J* = 2.6 Hz, 1 H), 8.71 (d, *J* = 2.5 Hz, 1 H), 8.39 (d, *J* = 2.2 Hz, 1 H), 8.20 (dd, *J* = 2.2, 8.8 Hz, 1 H), 7.59 (d, *J* = 8.8 Hz, 1 H).

*(S)-3-Bromo-7-iodo-5′H-spiro[chromeno[2,3-b]pyridine-5,4′-oxazol]-2′-amine (**12**).* Step 1: A mixture of 3-bromo-7-iodo-5*H*-chromeno[2,3-*b*]pyridin-5-one (33.0 g, 82 mmol) and THF (1642 mL, 82 mmol) in a 3 L three-neck flask was cooled to −40 °C. To this slurry was added methylmagnesium bromide (1 M in butyl ether) (164 mL, 164 mmol) via an addition funnel over 10 min. The internal temperature rose to −30 °C during the addition. The flask was maintained in the cooling bath and slowly allowed to warm to 0 °C over the course of 2 h. The reaction mixture was diluted with saturated aq ammonium chloride (1 L) and poured into a separatory funnel containing ethyl acetate (250 mL). The layers were separated, and the aqueous layer was extracted with ethyl acetate (2 × 250 mL). The combined organic layers were washed with brine, dried over sodium sulfate, filtered, and concentrated in vacuo (maintained on the rotovap at 80 °C for 30 min) to provide the tertiary alcohol as a light-yellow solid. The derived alcohol was taken up in 150 mL of THF and 50 mL of chloroform and maintained at 80 °C for 30 min. The yellow solid was concentrated under reduced pressure to give the crude olefin as an orange solid. The material was used directly in next step.

Step 2: A 2 L round-bottom flask charged with iodine (19.99 g, 79 mmol) and 600 mL of THF was cooled in a dry ice acetone bath until an internal temperature of −25 °C was maintained, at which point silver cyanate (33.7 g, 225 mmol) was added in one portion. During this addition, the internal temperature rose to −20 °C. The resulting slurry was maintained at between −25 and −20 °C for 20 min, at which point a solution of the crude 3-bromo-7-iodo-5-methylene-5*H*-chromeno[2,3-*b*]pyridine (30.0 g, 75.0 mmol) in 500 mL of THF was added via cannula over the course of 5 min. The internal temperature rose to −10 °C during this addition. The flask was recooled to −20 °C and maintained between −20 and −10 °C for 1.5 h. The reaction mixture was filtered through a plug of Celite (500 g) with the aid of diethyl ether (until the filtrate was colorless). The filtrate was concentrated in vacuo, and the resulting brown oily residue was taken up in THF (1 L). The resulting mixture was cooled to 0 °C and treated with ammonia (2 M in 2-propanol, 225 mL, 450 mmol). Following the addition, the flask was removed from the ice bath and maintained stirred for 8 h. The reaction mixture was diluted with 10% aq sodium thiosulfate solution (1 L) and poured into a separatory funnel containing ethyl acetate (500 mL) and brine (250 mL). The layers were separated, and the aqueous layer was extracted with ethyl acetate (2 × 500 mL). The combined organic layers were washed with brine, dried over sodium sulfate, filtered, and concentrated in vacuo to provide a brown residue. The residue was dried further by

dx.doi.org/10.1021/jm5012676 | J. Med. Chem. XXXX, XXX, XXX−XXX

concentration from toluene (3 × 100 mL). The residue was then triturated with DCM/MeOH (600 mL/300 mL) and cooled to 0 °C overnight. The mixture was then filtered. The solid was collected and the filtrate was concentrated, and the trituration procedure was repeated twice more. The collected solids were combined, and the filtrate was further purified by chromatography on silica gel (0−10% MeOH/DCM with 0.1% ammonium hydroxide). The product thus obtained was combined with solid to give 21.9 g of racemic (*S*)-3-bromo-7-iodo-5′*H*-spiro[chromeno[2,3-*b*]pyridine-5,4′-oxazol]-2′-amine. A portion of this material (16 g) was dissolved in a mixture of DCM (150 mL), MeOH (150 mL), and DMSO (25 mL). The solution was purified by SFC, using 6 mL injections on a 5 μm, 5 cm × 15 cm Chiralpak AD column with 35% MeOH/0.2% diethylamine/65% CO_2 at a flow rate of 250 mL/min. This afforded peak 1, (*R*)-3-bromo-7-iodo-5′*H*-spiro[chromeno[2,3-*b*]pyridine-5,4′-oxazol]-2′-amine (4.50 g, 9.82 mmol, 13.10% yield), and peak 2, (*S*)-3-bromo-7-iodo-5′*H*-spiro[chromeno[2,3-*b*]pyridine-5,4′-oxazol]-2′-amine (4.45 g, 9.72 mmol, 12.95% yield). ^{1}H NMR (400 MHz, DMSO-d_6) δ ppm 8.40 (d, J = 2.55 Hz, 1 H), 7.87 (d, J = 2.54 Hz, 1 H), 7.70 (dd, J = 8.56, 2.20 Hz, 1 H), 7.58 (d, J = 2.05 Hz, 1 H), 7.08 (d, J = 8.51 Hz, 1 H), 6.63 (s, 2 H), 4.16−4.30 (m, 2 H).

*(S)-3-Bromo-7-(2-fluoropyridin-3-yl)-5′H-spiro[chromeno[2,3-b]-pyridine-5,4′-oxazol]-2′-amine (**13**).* A 50 mL round-bottom flask was charged with (*S*)-3-bromo-7-iodo-5′*H*-spiro[chromeno[2,3-*b*]-pyridine-5,4′-oxazol]-2′-amine (2.56 g, 5.59 mmol), 2-fluoro-3-pyridineboronic acid (1.103 g, 7.82 mmol), potassium carbonate (2.317 g, 16.77 mmol), and 1,1′-bis(diphenylphosphino)ferrocene-palladium dichloride (0.228 g, 0.279 mmol). The flask was flushed with Ar(g), and then 1,4-dioxane (11.18 mL) and water (5.5 mL) were added in sequence. The flask was fitted with a reflux condenser and heated to 70 °C for 40 min. The mixture was cooled to room temperature and diluted with EtOAc (20 mL) and water (20 mL). The layers were separated, and the aqueous layer was extracted with EtOAc (20 mL). The organic layers were combined, and the combined solution was dried over sodium sulfate, filtered, and evaporated. The residue was purified by chromatography on silica gel (0−100% EtOAc/heptane) to give (*S*)-3-bromo-7-(2-fluoropyridin-3-yl)-5′*H*-spiro[chromeno[2,3-*b*]pyridine-5,4′-oxazol]-2′-amine (2.172 g, 5.08 mmol, 91% yield) as an orange solid. ^{1}H NMR (400 MHz, DMSO-d_6) δ = 8.42 (d, J = 2.4 Hz, 1 H), 8.29−8.21 (m, 1 H), 8.12 (ddd, J = 2.0, 7.4, 10.4 Hz, 1 H), 7.88 (d, J = 2.4 Hz, 1 H), 7.67−7.61 (m, 1 H), 7.57 (t, J = 1.8 Hz, 1 H), 7.49 (ddd, J = 2.0, 4.9, 7.5 Hz, 1 H), 7.38 (d, J = 8.6 Hz, 1 H), 6.58 (s, 2 H), 4.36−4.21 (m, 2 H). MS m/z = 427.0 $[M + H]^+$. Calcd for $C_{19}H_{13}BrFN_4O_2$: 427.0.

*3-Bromo-7-methoxy-5H-chromeno[2,3-b]pyridin-5-one (**15**).* Step 1: To a round-bottom flask charged with sodium hydride (60% dispersion in oil, 26.6 g, 666 mmol) was added *N*,*N*-dimethylformamide (634 mL, 317 mmol). The slurry was cooled to 0 °C and carefully treated with 4-methoxyphenol (39.4 g, 317 mmol) portionwise over 7 min, resulting in the evolution of a large amount of hydrogen gas. The mixture was stirred for 2 min, and then the ice bath was removed. After another 5 min of stirring, 5-bromo-2-chloronicotinic acid (75 g, 317 mmol) was slowly added portionwise over 5 min. After the addition was complete, the solution was heated to 140 °C for 1 h. The reaction mixture was cooled to room temperature and diluted with ice−water (750 mL). The brown mixture was acidified with acetic acid (91 mL, 1586 mmol), and then concentrate hydrochloric acid (93 mL, 1110 mmol) was added, resulting in the formation of a white precipitate. The pink slurry was stirred at room temperature for 2 h before being filtered to provide an off-white solid. This white solid contained residual DMF and was further dried under vacuum at 80 °C for 1 h to provide 5-bromo-2-(4-methoxyphenoxy)nicotinic acid (85.10 g, 263 mmol, 83% yield) as a white solid. ^{1}H NMR (400 MHz, chloroform-*d*) δ = 8.58 (d, J = 2.5 Hz, 1 H), 8.35 (d, J = 2.6 Hz, 1 H), 7.16−7.06 (m, 2 H), 7.02−6.92 (m, 2 H), 3.84 (s, 3 H).

Step 2: 5-Bromo-2-(4-methoxyphenoxy)nicotinic acid (85 g, 262 mmol) was added to a round-bottom flask containing polyphosphoric acid (900 g, 262 mmol) which had been heated to 140 °C. The mixture was maintained at 140 °C for 2 h and then cooled for 15 min. The partially cooled reaction mixture was poured onto 750 g of ice. The resulting mixture was then carefully adjusted with 10 M aq NaOH solution to a pH of 9−10 (during this quench the internal temperature rose to 100 °C). The mixture was cooled to room temperature and filtered. This material was taken up in DCM (200 mL), MeOH (200 mL), and benzene (100 mL). The mixture was concentrated in vacuo. The residue was taken up in DCM (400 mL) and MeOH (400 mL), and the resulting orange slurry was heated to 65 °C for 1 h, and then the hot solution was filtered. The filtrate was concentrated to afford 3-bromo-7-methoxy-5*H*-chromeno[2,3-*b*]pyridin-5-one (53.3 g, 174 mmol, 66.4% yield) as an orange solid. ^{1}H NMR (400 MHz, DMSO-d_6) δ = 8.94 (d, J = 2.6 Hz, 1 H), 8.72 (d, J = 2.6 Hz, 1 H), 7.77−7.70 (m, 1 H), 7.61−7.50 (m, 2 H), 3.90 (s, 3 H). MS m/z = 306.0 $[M + H]^+$. Calcd for $C_{13}H_9BrNO_3$: 306.0.

*(S)-3-Bromo-7-methoxy-5′H-spiro[chromeno[2,3-b]pyridine-5,4′-oxazol]-2′-amine (**16**).* Step 1: A three-neck 5 L flask equipped with an addition funnel and overhead stirrer was charged with 3-bromo-7-methoxy-5*H*-chromeno[2,3-*b*]pyridin-5-one (52.00 g, 170 mmol). THF (1.7 L) was added, and the reaction vessel was cooled in an ice bath. When the internal temperature reached 5 °C, methylmagnesium bromide (1 M in butyl ether) (340 mL, 340 mmol) was added dropwise via an addition funnel over the course of 15 min. The red slurry was removed from the ice bath and stirred at rt for 1.5 h. The reaction was carefully quenched with saturated aq ammonium chloride solution (1.2 L). DCM (1 L) was added, and the yellow mixture was stirred for 30 min. The layers were separated, and the aqueous layer was extracted with DCM (3 × 500 mL). The organic layers were each individually washed with brine and then combined. The combined solution was dried over sodium sulfate, filtered, and concentrated in vacuo at 75 °C provide an orange solid. The solid was suspended in MeOH (700 mL) and heated to 60 °C. The warm slurry was filtered to give 21.5 g of a light-yellow solid. The filtrate was concentrated, and the residue was purified by chromatgraphy on silica gel (eluting with DCM) to afford another 6.0 g of solid. The two solids were combined and dried under vacuum to give 3-bromo-7-methoxy-5-methylene-5*H*-chromeno[2,3-*b*]pyridine (27.5 g, 53% yield) as a light-yellow solid. ^{1}H NMR (400 MHz, DMSO-d_6) δ = 8.60 (d, J = 2.3 Hz, 1 H), 8.38 (d, J = 2.4 Hz, 1 H), 7.34 (d, J = 2.9 Hz, 1 H), 7.20 (d, J = 9.0 Hz, 1 H), 7.02 (dd, J = 2.9, 9.0 Hz, 1 H), 5.95 (d, J = 1.1 Hz, 1 H), 5.90 (d, J = 1.0 Hz, 1 H), 3.82 (s, 3 H),

Step 2: A round-bottom flask was charged with iodine (18.49 g, 72.8 mmol) and THF (347 mL, 69.4 mmol). The resulting solution was cooled to −15 °C and treated in one portion with silver isocyanate (31.2 g, 208 mmol). The temperature, which rose to −12 °C during the addition, was lowered to −20 °C and maintained for 15 min. A solution of 3-bromo-7-methoxy-5-methylene-5*H*-chromeno[2,3-*b*]-pyridine (21.10 g, 69.4 mmol) in THF (347 mL, 69.4 mmol) was added, and the resulting mixture was maintained at −20 to −10 °C for 1 h. The yellow slurry was diluted with ether (250 mL) and filtered through a pad of celilte, washing well with ether and THF. The resulting brown filtrate was concentrated under reduced pressure, with minimal heating. The derived brown oil was taken up in THF (347 mL, 69.4 mmol), cooled to 0 °C, and treated with ammonia (2 M in 2-PrOH) (104 mL, 208 mmol). The solution was maintained at 0 °C for 15 min then warmed to room temperature, where it was maintained for 10 h. The reaction was diluted with 10% aq sodium thiosulfate solution (1 L) and poured into a separatory funnel containing EtOAc (250 mL). The layers were separated, and the aq layer was extracted with EtOAc (3 × 250 mL). The combined organic extracts were washed with brine, dried over sodium sulfate, filtered, and concentrated in vacuo. The residue was purified by silical gel chromatography (0−100% EtOAc/hexanes) to provide *rac*-3-bromo-7-methoxy-5′*H*-spiro[chromeno[2,3-*b*]pyridine-5,4′-oxazol]-2′-amine (17.5 g, 48.3 mmol, 69.6% yield) as a yellow solid. This material was dissolved in 1:1 DCM/MeOH (300 mL), and the resulting solution was purified by SFC, using 4 mL injections on a 5 cm × 25 cm Chiralpak AD-H column with 35% MeOH/0.2% diethylamine/65% CO_2 at a flow rate of 250 mL/min to give peak 1, (*R*)-3-bromo-7-methoxy-5′*H*-spiro[chromeno[2,3-*b*]pyridine-5,4′-oxazol]-2′-amine (6.47 g), and peak 2, (*S*)-3-bromo-7-methoxy-5′*H*-spiro[chromeno-

dx.doi.org/10.1021/jm5012676 | J. Med. Chem. XXXX, XXX, XXX−XXX

[2,3-*b*]pyridine-5,4′-oxazol]-2′-amine (7.12 g, 28% yield). Data for peak 2: ^{1}H NMR (400 MHz, DMSO-d_6) δ = 8.37 (d, J = 2.5 Hz, 1 H), 7.83 (d, J = 2.4 Hz, 1 H), 7.18 (d, J = 8.9 Hz, 1 H), 6.96 (dd, J = 3.1, 8.9 Hz, 1 H), 6.81 (d, J = 2.9 Hz, 1 H), 6.58 (br s, 2 H), 4.32−4.12 (m, 2 H), 3.76 (s, 3 H).

*(S)-2′-Amino-3-bromo-5′H-spiro[chromeno[2,3-b]pyridine-5,4′-oxazol]-7-ol (**17**).* A 250 mL round-bottom flask was charged with a solution of (*S*)-3-bromo-7-methoxy-5′*H*-spiro[chromeno[2,3-*b*]-pyridine-5,4′-oxazol]-2′-amine (1.832 g, 5.06 mmol) in DCM (50.6 mL). The flask was cooled in an ice-bath for 10 min, and then BBr_3 (1.913 mL, 20.23 mmol) was added over 30 s, slightly faster than dropwise. The mixture was stirred for 5 min, and then the ice-bath was removed. The mixture was stirred for 5 h at room temperature and then was diluted with saturated aq sodium bicarbonate solution (75 mL). A solid formed, so THF (30 mL) was added and the mixture was stirred overnight. The layers were separated, and the aqueous layer was extracted with DCM (3 × 50 mL). The combined organic extracts were dried over sodium sulfate, filtered, and evaporated to give an orange solid. The solid was taken up in DCM (50 mL), and the resulting mixture was sonicated for 10 min. The mixture was then cooled in an ice-bath for 20 min. The solid was filtered, washed with cold DCM (30 mL), and dried under vacuum to give give (*S*)-2′-amino-3-bromo-5′*H*-spiro[chromeno[2,3-*b*]pyridine-5,4′-oxazol]-7-ol (1.089 g, 3.13 mmol, 61.8% yield) as a cream-colored solid. MS m/z = 347.8 $[M + H]^+$. Calcd for $C_{14}H_{11}BrN_3O_3$: 348.0.

*3-Bromo-7-hydroxy-spiro[chromeno[2,3-b]pyridine]-5,4′-[1,3]-oxazole]-2′-amine (rac-**17**).* To a solution of *rac*-3-bromo-7-methoxy-spiro[chromeno[2,3-*b*]pyridine]-5,4′-[1,3]oxazole]-2′-amine (2300 mg, 6350 μmol) in DCM (12.7 mL 6.35 mmol) at 0 °C was added BBr_3 (1.8 mL, 19 mmol). Immediately a thick precipitate formed. The resulting red slurry was stirred at 0 °C for 10 min, at which point the ice bath was removed and the mixture was allowed to warm to rt and stirred at rt for 1 h. Another portion of BBr_3 (1 mL) at 23 °C, and the mixture was stirred for 1 h. The reaction was cooled to 0 °C and carefully quenched with saturated aq sodium bicarbonate solution (250 mL) and then poured into DCM (250 mL). The layers were separated, and the aqueous layer was extracted with DCM (3 × 300 mL). The organic layers were washed with brine, dried over Na_2SO_4, and filtered. The extraction process was repeated with DCM. All organic layers were combined and concentrated under reduced pressure to provide 3-bromo-7-hydroxy-spiro[chromeno[2,3-*b*]-pyridine]-5,4′-[1,3]oxazole]-2′-amine (2.2 g, 99% yield) as a brown solid. MS m/z = 348.0 $[M + H]^+$. Calcd for $C_{14}H_{11}BrN_3O_3$: 348.0.

*(S)-2′-Amino-3-(tetrahydro-2H-pyran-4-yl)-5′H-spiro[chromeno-[2,3-b]pyridine-5,4′-oxazol]-7-ol (**18a**).* Step 1: A vial was charged with (*S*)-2′-amino-3-bromo-5′*H*-spiro[chromeno[2,3-*b*]pyridine-5,4′-oxazol]-7-ol (380 mg, 1.091 mmol), potassium carbonate (754 mg, 5.46 mmol), 2-(3,6-dihydro-2*H*-pyran-4-yl)-4,4,5,5-tetramethyl-1,3,2-dioxaborolane (688 mg, 3.27 mmol), $Pd(Ph_3P)_4$ (126 mg, 0.109 mmol), DMF (5457 μL), and water (2.5 mL). The vial was sealed and heated to 80 °C overnight. The mixture was diluted with water (35 mL) and extracted with EtOAc (3 × 15 mL). The combined organic extracts were dried over sodium sulfate, filtered, and evaporated. The residue was purified by chromatography on silica gel (0−100% of a 90:10:1 mix of DCM/MeOH/NH_4OH in DCM) to give give (*S*)-2′-amino-3-(3,6-dihydro-2*H*-pyran-4-yl)-5′*H*-spiro[chromeno[2,3-*b*]-pyridine-5,4′-oxazol]-7-ol (267.7 mg, 0.762 mmol, 69.8% yield) as an orange solid. MS m/z = 352.0 $[M + H]^+$. Calcd for $C_{19}H_{18}N_3O_4$: 352.1.

Step 2: A 25 mL flask was charged with (*S*)-2′-amino-3-(3,6-dihydro-2*H*-pyran-4-yl)-5′*H*-spiro[chromeno[2,3-*b*]pyridine-5,4′-oxazol]-7-ol (211 mg, 0.601 mmol) and MeOH (7.5 mL). The mixture was sonicated for 1 min to give an opaque mixture. 10% Pd/C (63.9 mg, 0.060 mmol) was added, and H_2(g) was bubbled through the mixture for 1 min. The mixture was stirred further under a balloon of H_2(g) for 24 h. H_2(g) was again bubbled in for 1 min, and the mixture was stirred for 2 days under a H_2(g) balloon. The mixture was filtered through Celite with the aid of methanol. The filtrate was evaporated, and the residue was purified by chromatography on silica gel (0−100% of a 90:10:1 mix of DCM/MeOH/NH_4OH) to give (*S*)-2′-amino-3-(tetrahydro-2*H*-pyran-4-yl)-5′*H*-spiro[chromeno[2,3-*b*]pyridine-5,4′-oxazol]-7-ol (201.8 mg, 0.698 mmol, 82% yield) as an off-white solid. ^{1}H NMR (400 MHz, DMSO-d_6) δ = 9.31 (s, 1 H), 8.13 (d, J = 2.3 Hz, 1 H), 7.60 (d, J = 2.4 Hz, 1 H), 7.09−6.97 (m, 1 H), 6.81−6.68 (m, 2 H), 6.48 (s, 2 H), 4.16−4.08 (m, 2 H), 3.95 (dd, J = 1.9, 9.5 Hz, 2 H), 3.48−3.38 (m, 2 H), 2.91−2.78 (m, 1 H), 1.77−1.56 (m, 4 H). MS m/z = 354.0 $[M + H]^+$. Calcd for $C_{19}H_{20}N_3O_4$: 354.2.

*(S)-2′-Amino-3-(6,6-dimethyl-3,6-dihydro-2H-pyran-4-yl)-5′H-spiro[chromeno[2,3-b]pyridine-5,4′-oxazol]-7-ol (**18b**).* A microwave reaction vial was charged with (*S*)-2′-amino-3-bromo-5′*H*-spiro-[chromeno[2,3-*b*]pyridine-5,4′-oxazol]-7-ol (0.850 g, 2.441 mmol), 2-(2,2-dimethyl-3,6-dihydro-2*H*-pyran-4-yl)-4,4,5,5-tetramethyl-1,3,2-dioxaborolane (as a 1.5:1 mixture of olefin isomers, 0.930 g, 3.91 mmol), potassium carbonate (1.012 g, 7.32 mmol) and $PdCl_2(AmPhos)_2$ (0.086 g, 0.122 mmol), 1,4-dioxane (14.24 mL), and water (2.035 mL). The vial was sealed and heated in microwave reactor for 1 h at 100 °C. The reaction mixture was diluted with water and washed with EtOAc. The aqueous layer was extracted with EtOAc, and the combined organic layers were dried with sodium sulfate, filtered, and concentrated. The residue was purified via column chromatography on silica gel (0−80% of a 90:10:1 mixture of DCM/MeOH/NH_4OH in DCM). The resulting material was repurified to collect the title regiosomer as the first eluting peak to afford (*S*)-2′-amino-3-(6,6-dimethyl-3,6-dihydro-2*H*-pyran-4-yl)-5′*H*-spiro-[chromeno[2,3-*b*]pyridine-5,4′-oxazol]-7-ol (0.604 g, 1.592 mmol, 65.2% yield) as a tan solid. ^{1}H NMR (400 MHz, DMSO-d_6) δ = 9.35 (br s, 1 H), 8.31 (d, J = 2.4 Hz, 1 H), 7.73 (d, J = 2.4 Hz, 1 H), 7.08−7.00 (m, 1 H), 6.83−6.69 (m, 2 H), 6.50 (s, 2 H), 6.17 (t, J = 1.5 Hz, 1 H), 4.14 (s, 2 H), 3.83 (t, J = 5.4 Hz, 2 H), 2.40−2.32 (m, 2 H), 1.27 (s, 3 H), 1.27 (s, 3 H). MS m/z = 380.2 $[M + H]^+$. Calcd for $C_{21}H_{22}N_3O_4$: 380.2.

*(S)-2′-Amino-3-morpholino-5′H-spiro[chromeno[2,3-b]pyridine-5,4′-oxazol]-7-ol (**18c**).* A vial was charged with (*S*)-2′-amino-3-bromo-5′*H*-spiro[chromeno[2,3-*b*]pyridine-5,4′-oxazol]-7-ol (0.647 g, 1.858 mmol), DavePhos (0.088 g, 0.223 mmol), and tris-(dibenzylideneacetone)dipalladium(0) (0.085 g, 0.093 mmol). The vessel was flushed with Ar(g), and then lithium bis(trimethylsilyl)-amide (1.0 M in THF) (9.29 mL, 9.29 mmol) and morpholine (0.486 mL, 5.58 mmol) were added in sequence. The vial was sealed and heated at 70 °C for 1 h. The mixture was diluted with water and saturated aq ammoniom chloride solution. The mixture was extracted with DCM (3 × 30 mL) and EtOAc (3×). The combined organic extracts were combined, dried over sodium sulfate, filtered, and evaporated. The residue was purified by chromatography on silica gel (0−10% of a 90:10:1 mix of DCM/MeOH/NH_4OH in DCM) to afford (*S*)-2′-amino-3-morpholino-5′*H*-spiro[chromeno[2,3-*b*]-pyridine-5,4′-oxazol]-7-ol (0.336 g, 0.948 mmol, 51.0% yield) as an orange solid. MS m/z = 355.2 $[M + H]^+$. Calcd for $C_{18}H_{19}N_4O_4$: 355.1.

*(S)-2′-Amino-3-(p-tolyl)-5′H-spiro[chromeno[2,3-b]pyridine-5,4′-oxazol]-7-ol (**18d**).* A vial was charged (*S*)-2′-amino-3-bromo-5′*H*-spiro[chromeno[2,3-*b*]pyridine-5,4′-oxazol]-7-ol (282 mg, 0.809 mmol), *p*-tolylboronic acid (220 mg, 1.618 mmol), potassium carbonate (559 mg, 4.04 mmol), and $Pd(Ph_3P)_4$ (46.7 mg, 0.040 mmol). The vial was flushed with Ar(g), and then 1,4-dioxane (4 mL) and water (2 mL) were added in sequence. The vial was sealed and heated to 80 °C for 1.5 h. The mixture was partitioned between brine and 10% iPrOH/EtOAc. The layers were separated, and the aqueous layer was extracted with EtOAc. The combined organic extracts were dried over sodium sulfate, filtered, and evaporated. The residue was purified by chromatography on silica gel (0−80% of a 90:10:1 mix of DCM/MeOH/NH_4OH in DCM) to give (*S*)-2′-amino-3-*p*-tolyl-5′*H*-spiro[chromeno[2,3-*b*]pyridine-5,4′-oxazol]-7-ol (259.36 mg, 0.722 mmol, 89% yield) as an orange solid. MS m/z = 360.0 $[M + H]^+$. Calcd for $C_{21}H_{18}N_3O_3$: 360.1.

*(S)-4-(2′-Amino-7-hydroxy-5′H-spiro[chromeno[2,3-b]pyridine-5,4′-oxazol]-3-yl)benzonitrile (**18e**).* A vial was charged with (*S*)-2′-amino-3-bromo-5′*H*-spiro[chromeno[2,3-*b*]pyridine-5,4′-oxazol]-7-ol (247 mg, 0.711 mmol), 4-cyanophenylboronic acid (313 mg, 2.132 mmol), potassium carbonate (491 mg, 3.55 mmol), and $Pd(Ph_3P)_4$

dx.doi.org/10.1021/jm5012676 | J. Med. Chem. XXXX, XXX, XXX−XXX

(82 mg, 0.071 mmol). The vial was flushed with Ar(g), and then 1,4-dioxane (3553 μL) and water (1.8 mL) were added in sequence. The vial was sealed and heated to 80 °C overnight. The next morning, the mixture was diluted with water (40 mL) and extracted with EtOAc (3 × 20 mL). The combined organic extracts were dried over sodium sulfate, filtered, and evaporated. The residue was purified by chromatography on silica gel (0−9% MeOH/DCM) to give (*S*)-4-(2′-amino-7-hydroxy-5′*H*-spiro[chromeno[2,3-*b*]pyridine-5,4′-oxazole]-3-yl)benzonitrile (181.62 mg, 0.490 mmol, 69.0% yield) as a yellow solid. ^{1}H NMR (400 MHz, DMSO-d_6) δ = 9.39 (s, 1 H), 8.65 (d, J = 2.5 Hz, 1 H), 8.05 (d, J = 2.4 Hz, 1 H), 8.00−7.86 (m, 4 H), 7.14−7.03 (m, 1 H), 6.81−6.70 (m, 2 H), 6.50 (br s, 2 H), 4.31−4.25 (m, 1 H), 4.23−4.18 (m, 1 H). MS m/z = 371.0 [M + H]$^+$. Calcd for $C_{21}H_{15}N_4O_3$: 371.1.

*(S)-2′-Amino-3-(tetrahydro-2H-pyran-4-yl)-5′H-spiro[chromeno-[2,3-b]pyridine-5,4′-oxazol]-7-yl Trifluoromethanesulfonate (**19a**).* A 25 mL round-bottom flask was charged with (*S*)-2′-amino-3-(tetrahydro-2*H*-pyran-4-yl)-5′*H*-spiro[chromeno[2,3-*b*]pyridine-5,4′-oxazol]-7-oland triethylamine (194 μL, 1.392 mmol) in DCM (2.5 mL) to give an opaque mixture. *N*-Phenyltrifluoromethanesulfonimide (261 mg, 0.731 mmol) was added, and the resulting mixture was stirred for 24 h. An additional portion of *N*-phenyltrifluoromethanesulfonimide (50 mg) was added, and the mixture was stirred for an additional 4 h. The reaction mixture was diluted with DCM (20 mL) and saturated aq sodium bicarbonate solution (20 mL). The layers were separated, and the aqueous layer was extracted with DCM (2 × 10 mL). The combined organic extracts were dried over sodium sulfate, filtered, and evaporated. The residue was purified by chromatography on silica gel (0−7% MeOH/DCM) to give (*S*)-2′-amino-3-(tetrahydro-2*H*-pyran-4-yl)-5′*H*-spiro[chromeno[2,3-*b*]-pyridine-5,4′-oxazole]-7-yl trifluoromethanesulfonate (280.69 mg, 0.578 mmol, 83% yield) as a white solid. ^{1}H NMR (400 MHz, DMSO-d_6) δ = 8.22 (d, J = 2.3 Hz, 1 H), 7.68 (br s, 1 H), 7.57−7.50 (m, 1 H), 7.46−7.41 (m, 1 H), 7.36 (br s, 1 H), 4.24 (br s, 2 H), 3.96 (dd, J = 1.7, 11.2 Hz, 2 H), 3.44 (tt, J = 2.5, 11.2 Hz, 2 H), 2.96−2.81 (m, 1 H), 1.75−1.59 (m, 4 H). MS m/z = 485.8 [M + H]$^+$. Calcd for $C_{20}H_{19}F_3N_3O_6S$: 486.1.

*(S)-2′-Amino-3-(6,6-dimethyl-3,6-dihydro-2H-pyran-4-yl)-5′H-spiro[chromeno[2,3-b]pyridine-5,4′-oxazol]-7-yl Trifluoromethanesulfonate (**19b**).* (*S*)-2′-Amino-3-(6,6-dimethyl-3,6-dihydro-2*H*-pyran-4-yl)-5′*H*-spiro[chromeno[2,3-*b*]pyridine-5,4′-oxazol]-7-ol (0.231 g, 0.609 mmol) and triethylamine (0.255 mL, 1.827 mmol) were combined in DCM (12.18 mL). 1,1,1-Trifluoro-*N*-phenyl-*N*-(trifluoromethylsulfonyl)methanesulfonamide (0.239 g, 0.670 mmol) was added, and the solution was stirred at room temperature overnight. In the morning, the solution purified directly by chromatography on silica gel (0−60% of a 90:10:1 mixture of DCM/MeOH/NH_4OH in DCM) to afford (*S*)-2′-amino-3-(6,6-dimethyl-3,6-dihydro-2*H*-pyran-4-yl)-5′*H*-spiro[chromeno[2,3-*b*]-pyridine-5,4′-oxazole]-7-yl trifluoromethanesulfonate (0.258 g, 0.504 mmol, 83% yield) as a off-white solid. ^{1}H NMR (400 MHz, DMSO-d_6) δ = 8.38 (d, J = 2.4 Hz, 1 H), 7.78 (s, 1 H), 7.54 (dd, J = 3.0, 9.0 Hz, 1 H), 7.48−7.40 (m, 1 H), 7.32 (br s, 1 H), 6.65 (br s, 2 H), 6.23 (s, 1 H), 4.33−4.12 (m, 2 H), 3.84 (t, J = 5.4 Hz, 2 H), 2.41−2.34 (m, 2 H), 1.28 (s, 6 H). MS m/z = 512.1 [M + H]$^+$. Calcd for $C_{22}H_{21}F_3N_3O_6S$: 512.1.

*(S)-2′-Amino-3-morpholino-5′H-spiro[chromeno[2,3-b]pyridine-5,4′-oxazol]-7-yl Trifluoromethanesulfonate (**19c**).* A 25 mL round-bottom flask was charged with cesium carbonate (0.371 g, 1.138 mmol), (*S*)-2′-amino-3-morpholino-5′*H*-spiro[chromeno[2,3-*b*]-pyridine-5,4′-oxazol]-7-ol (0.336 g, 0.948 mmol), and DMF (4.74 mL). The resulting mixture was stirred for 10 min, and then the flask was submerged in an ice bath for 5 min. *N*-Phenyltrifluoromethanesulfonimide (0.373 g, 1.043 mmol) was added as a single portion, and the reaction was stirred overnight, during which the ice bath was allowed to melt. In the morning, the mixture was cooled to 0 °C, and additional portions of cesium carbonate (150 mg) and *N*-phenyltrifluoromethanesulfonimide were added in sequence. The mixture was stirred for an additional 1 h and then was diluted with water and extracted with EtOAc (2×). The combined organic extracts were dried over sodium sulfate, filtered, and evaporated. The residue was purified by chromatography on silica gel (0−70% of a 90:10:1 mix of DCM/MeOH/NH_4OH in DCM) to afford (*S*)-2′-amino-3-morpholino-5′*H*-spiro[chromeno[2,3-*b*]pyridine-5,4′-oxazole]-7-yl trifluoromethanesulfonate (0.309 g, 0.635 mmol, 67% yield) as an off-white solid. The material was about 80% pure as determined by LCMS and was used directly in the next reaction. MS m/z = 487.2 [M + H]$^+$. Calcd for $C_{19}H_{18}F_3N_4O_6S$: 487.1.

*(S)-2′-Amino-3-(p-tolyl)-5′H-spiro[chromeno[2,3-b]pyridine-5,4′-oxazol]-7-yl Trifluoromethanesulfonate (**19d**).* A 25 mL flask was charged with (*S*)-2′-amino-3-*p*-tolyl-5′*H*-spiro[chromeno[2,3-*b*]-pyridine-5,4′-oxazol]-7-ol (259.36 mg, 0.722 mmol) in DCM (7217 μL) to give an clear, orange solution. Triethylamine (201 μL, 1.443 mmol) and 1,1,1-trifluoro-*N*-phenyl-*N*-(trifluoromethylsulfonyl)-methanesulfonamide (271 mg, 0.758 mmol) were added in sequence. The resulting mixture was stirred for 3 h and then was purified directly by chromatography on silica gel (0−5% MeOH/DCM) to give (*S*)-2′-amino-3-*p*-tolyl-5′*H*-spiro[chromeno[2,3-*b*]pyridine-5,4′-oxazole]-7-yl trifluoromethanesulfonate (317.34 mg, 0.646 mmol, 89% yield) as a cream-colored solid. ^{1}H NMR (400 MHz, DMSO-d_6) δ = 8.58 (d, J = 2.4 Hz, 1 H), 7.96 (d, J = 2.4 Hz, 1 H), 7.64−7.52 (m, 2 H), 7.49−7.43 (m, 1 H), 7.37−7.30 (m, 2 H), 6.66 (br s, 2 H), 4.40−4.16 (m, 2 H), 2.36 (s, 3 H). MS m/z = 492.0 [M + H]$^+$. Calcd for $C_{22}H_{17}F_3N_3O_5S$: 492.0.

*(S)-2′-Amino-3-(4-cyanophenyl)-5′H-spiro[chromeno[2,3-b]-pyridine-5,4′-oxazol]-7-yl Trifluoromethanesulfonate (**19e**).* A round-bottom flask was charged with (*S*)-4-(2′-amino-7-hydroxy-5′*H*-spiro[chromeno[2,3-*b*]pyridine-5,4′-oxazole]-3-yl)benzonitrile (181.62 mg, 0.490 mmol) and DCM (4904 μL) to give a suspension. Triethylamine (137 μL, 0.981 mmol) was added, and the starting material dissolved after a few minutes of stirring. *N*-Phenylbis(trifluoromethanesulfonimide) (184 mg, 0.515 mmol) was added, and the mixture was stirred overnight. In the morning, the reaction mixture was diluted with saturated aq sodium bicarbonate solution (20 mL). The layers were separated, and the aqueous layer was extracted with DCM (2 × 20 mL). The combined organic extracts were dried over sodium sulfate, filtered, and evaporated. The residue was purified by chromatography on silica gel (0−5% MeOH/DCM) to give (*S*)-2′-amino-3-(4-cyanophenyl)-5′*H*-spiro[chromeno[2,3-*b*]pyridine-5,4′-oxazole]-7-yl trifluoromethanesulfonate (186.48 mg, 0.371 mmol, 76% yield) as an off-white solid. ^{1}H NMR (400 MHz, DMSO-d_6) δ = 8.71 (d, J = 2.5 Hz, 1 H), 8.10 (d, J = 2.4 Hz, 1 H), 8.03−7.89 (m, 4 H), 7.59−7.53 (m, 1 H), 7.51−7.45 (m, 1 H), 7.34 (d, J = 2.9 Hz, 1 H), 6.65 (s, 2 H), 4.38 (d, J = 8.8 Hz, 1 H), 4.27 (d, J = 8.8 Hz, 1 H). MS m/z = 502.8 [M + H]$^+$. Calcd for $C_{22}H_{14}F3N_4O_5S$: 503.1.

*7-Bromo-3-iodo-5H-chromeno[2,3-b]pyridin-5-one (**21**).* Step 1: 2-(4-Bromophenoxy)-5-iodonicotinic acid. A solution of 2,2,6,6-tetramethylpiperidine (45.7 mL, 269 mmol) in THF (400 mL) was cooled to −10 °C and then treated with *n*-butyllithium (103 mL, 257 mmol). After stirring for 10 min, the reaction mixture was cooled to −78 °C. The cooled solution was treated with a solution of 2-fluoro-5-iodopyridine (54.6 g, 245 mmol) in THF (200 mL). The reaction mixture was stirred for 40 min, and then CO_2 (g) gas was bubbled through for 10 min via syringe. The reaction mixture was placed in a 0 °C bath, and CO_2(g) was bubbled through for an additional 10 min. 4-Bromophenol (46.6 g, 269 mmol) and potassium carbonate (42.3 g, 306 mmol) were added in sequence. The reaction mixture was concentrated in vacuo, and the residue was suspended in DMF (500 mL). The resulting mixture was heated to 140 °C overnight. In the morning, the mixture was cooled to room temperature and then poured into 1N aq HCl. The resulting suspension was filtered, washed with 1:1 water/acetone, and dried to give 2-(4-bromophenoxy)-5-iodonicotinic acid (92.60 g, 220 mmol, 90% yield). ^{1}H NMR (400 MHz, acetonitrile-d_3) δ = 8.52 (d, J = 2.3 Hz, 1 H), 8.42 (d, J = 2.3 Hz, 1 H), 7.58−7.52 (m, 2 H), 7.08−7.04 (m, 2 H). MS m/z = 419.8 [M + H]$^+$. Calcd for $C_{12}H_8BrINO$: 419.9.

Step 2: 7-Bromo-3-iodo-5*H*-chromeno[2,3-*b*]pyridin-5-one. A flask charged with 2-(4-bromophenoxy)-5-iodonicotinic acid (93 g, 220 mmol) and polyphosphoric acid 115% (926 g, 220 mmol) was heated to 120 °C overnight. In the morning, starting material persisted, so the

dx.doi.org/10.1021/jm5012676 | J. Med. Chem. XXXX, XXX, XXX−XXX

reaction mixture was heated to 140 °C for 3 h. The reaction mixture was then cooled to room temperature and poured into water. The water slurry was stirred for 2 h and then filtered. The collected solid was washed with 1N aq NaOH, water, and 2-PrOH, then dried under air to yield 7-bromo-3-iodo-5*H*-chromeno[2,3-*b*]pyridin-5-one (63.48 g, 158 mmol, 71.6% yield). ^{1}H NMR (400 MHz, chloroform-*d*) δ = 8.98 (d, *J* = 2.4 Hz, 1 H), 8.94 (d, *J* = 2.4 Hz, 1 H), 8.44 (d, *J* = 2.4 Hz, 1 H), 7.89 (dd, *J* = 2.4, 8.9 Hz, 1 H), 7.53 (d, *J* = 9.0 Hz, 1 H). MS *m*/*z* = 401.7 [M + H]$^+$. Calcd for $C_{12}H_6BrINO_2$: 401.7.

*7-Bromo-3-hydroxy-5H-chromeno[2,3-b]pyridin-5-one (**22**).* A flask charged with $Pd(OAc)_2$ (1.773 g, 7.90 mmol), X-Phos (11.29 g, 23.69 mmol), 7-bromo-3-iodo-5*H*-chromeno[2,3-*b*]pyridin-5-one (63.5 g, 158 mmol), bis(pinacolato)diboron (42.1 g, 166 mmol), and potassium phosphate (101 g, 474 mmol) was diluted with 1,4-dioxane (600 mL), and the resulting mixture was stirred at room temperature overnight. The reaction mixture was filtered through a plug of Celite, and the filtrate was diluted with THF (500 mL) and a 6N aq sodium hydroxide solution (132 mL, 790 mmol). The resulting mixture was cooled to 0 °C, and hydrogen peroxide 30% (58.1 mL, 1895 mmol) was added dropwise. The resulting mixture was stirred for 5 h and then diluted with MeOH (500 mL). A 6N aq hydrochloric acid solution (150 mL) and a 10% aq sodium thiosulfate solution (300 mL) were added in sequence. The mixture was then concentrated in vacuo to remove the volatiles, and the resulting suspension was filtered. The collected solid was washed with 1:1 water/acetone and dried. The resulting dark-brown solid was triturated with warm diethyl ether then hot acetonitrile and then filtered to give 7-bromo-3-hydroxy-5*H*-chromeno[2,3-*b*]pyridin-5-one (30.39 g, 104 mmol, 65.9% yield). ^{1}H NMR (400 MHz, chloroform-*d*) δ = 8.43 (d, *J* = 2.2 Hz, 1 H), 8.32 (d, *J* = 2.8 Hz, 1 H), 8.03 (d, *J* = 2.7 Hz, 1 H), 7.83 (dd, *J* = 2.4, 8.8 Hz, 1 H), 7.54−7.47 (m, 1 H), 7.00 (s, 1 H). MS *m*/*z* = 291.9 [M + H]$^+$. Calcd for $C_{12}H_7BrNO_3$: 291.9.

*rac-7-Bromo-3-(2-methoxy-2-methylpropoxy)-5-methyl-5H-chromeno[2,3-b]pyridin-5-ol (**23**).* Step 1: A solution of 7-bromo-3-hydroxy-5*H*-chromeno[2,3-*b*]pyridin-5-one (15.00 g, 51.4 mmol) in DCM (100 mL) was treated with DBU (9.68 mL, 64.2 mmol) and stirred for 10 min. 3-Bromo-2-methylpropene (5.44 mL, 53.9 mmol) was added, and the resulting mixture was stirred for an additional hour. The reaction mixture was quenched with 0.5 N aq citric acid solution (200 mL) and concentrated in vacuo to remove the volatiles. The resulting suspension was filtered, and the collected solid was washed with 1:1 water/acetone and dried. The solid was purified by chromatography on silica gel (0−50% EtOAc/hexane), yielding 7-bromo-3-(2-methylallyloxy)-5*H*-chromeno[2,3-*b*]pyridin-5-one (4.50 g, 13.00 mmol, 25.3% yield). ^{1}H NMR (400 MHz, acetonitrile-d_3) δ = 8.51 (d, *J* = 3.2 Hz, 1 H), 8.34 (d, *J* = 2.5 Hz, 1 H), 8.06 (d, *J* = 3.3 Hz, 1 H), 7.95 (dd, *J* = 2.5, 8.9 Hz, 1 H), 7.59 (d, *J* = 8.9 Hz, 1 H), 5.15 (d, *J* = 0.7 Hz, 1 H), 5.06 (d, *J* = 1.6 Hz, 1 H), 4.67 (s, 2 H), 1.85 (d, *J* = 0.5 Hz, 3 H). MS *m*/*z* = 346.0 [M + H]$^+$. Calcd for $C_{16}H_{13}BrNO_3$: 346.0.

Step 2: A suspension of 7-bromo-3-((2-methylallyl)oxy)-5*H*-chromeno[2,3-*b*]pyridin-5-one (2.420 g, 6.99 mmol) in MeOH (100 mL) was treated with *N*-iodosuccinimide (7.86 g, 35.0 mmol), and the resulting mixture was stirred at room temperature for 36 h. The crude product was purified by chromatography on silica gel (0−100% EtOAc/hexane) to give 7-bromo-3-(3-iodo-2-methoxy-2-methylpropoxy)-5*H*-chromeno[2,3-*b*]pyridin-5-one (2.33 g, 4.62 mmol, 66.1% yield) as an oil. ^{1}H NMR (400 MHz, acetonitrile-d_3) δ = 8.52 (d, *J* = 3.3 Hz, 1 H), 8.34 (d, *J* = 2.4 Hz, 1 H), 8.13−8.10 (m, 1 H), 7.95 (dd, *J* = 2.5, 8.9 Hz, 1 H), 7.60 (d, *J* = 9.0 Hz, 1 H), 4.24−4.07 (m, 2 H), 3.62−3.52 (m, 2 H), 3.27 (s, 3 H), 1.45 (s, 3 H). MS *m*/*z* = 503.9 [M + H]$^+$. Calcd for $C_{17}H_{16}BrINO_4$: 503.9.

Step 3: A solution of 7-bromo-3-(3-iodo-2-methoxy-2-methylpropoxy)-5*H*-chromeno[2,3-*b*]pyridin-5-one (4.10 g, 8.13 mmol) in THF (100 mL) cooled to −40 °C was treated with methylmagnesium chloride (5.42 mL of 3 M solution in diethyl ether, 16.27 mmol). After stirring for 2 h, the reaction mixture was allowed to warm to room temperature. Lithium triethylborohydride (40.7 mL of a 1 M solution in THF, 40.7 mmol) was added added over 5 min. After stirring for an additional 2 h at room temperature, the reaction mixture was cooled to 0 °C and was quenched with MeOH. The reaction mixture was poured into saturated aq ammonium chloride solution and extracted with EtOAc. The organic layer was washed with water and brine, dried over $MgSO_4$, and concentrated, yielding crude 7-bromo-3-(2-methoxy-2-methylpropoxy)-5-methyl-5*H*-chromeno[2,3-*b*]pyridin-5-ol (1.80 g, 4.57 mmol, 56.1% yield). This material was used directly in the next reaction. MS *m*/*z* = 394.0 [M + H]$^+$. Calcd for $C_{18}H_{21}BrNO_4$: 394.0.

*rac-7-Bromo-3-(2-methoxy-2-methylpropoxy)-5′H-spiro-[chromeno[2,3-b]pyridine-5,4′-oxazol]-2′-amine (**24**).* A solution of 7-bromo-3-(2-methoxy-2-methylpropoxy)-5-methyl-5*H*-chromeno-[2,3-*b*]pyridin-5-ol (1.780 g, 4.51 mmol) in THF (50 mL) was treated with a 4 M HCl solution in 1,4-dioxane (0.113 mL, 0.451 mmol), and the resulting mixture was heated to 50 °C for 1 h to afford a solution containing the corresponding olefin. The solution was cooled to 0 °C. Separately, silver cyanate (1.692 g, 11.29 mmol) was added in one portion to a solution of iodine (1.260 g, 4.97 mmol) in THF (50 mL) maintained at −40 °C. The resulting was stirred for 1 h at −40 °C, and then the solution of olefin was via cannula. After an additional hour of stirring, ammonia (13.54 mL of 2 M solution in 2-PrOH) was added in one portion. The mixture was warmed to room temperature and stirred for a further 3 h. The reaction mixture was quenched with a 10% aq sodium thiosulfate solution, and the resulting biphasic mixture was stirred at room temperature for 1 h. The organic layer was separated, washed with water, washed with brine, dried over $MgSO_4$, filtered, and concentrated. The crude product was purified by chromatography on silica gel (0−10% MeOH/DCM) to give *rac*-bromo-3-(2-methoxy-2-methylpropoxy)-5′*H*-spiro[chromeno[2,3-*b*]-pyridine-5,4′-oxazol]-2′-amine (0.319 g, 0.735 mmol, 16.27% yield) as an off-white solid. MS *m*/*z* = 434.0 [M + H]$^+$. Calcd for $C_{19}H_{21}BrN_3O_4$: 434.0.

*3-Bromo-7-(2,2-dimethylpropoxy)-spiro[chromeno[2,3-b]-pyridine]-5,4′-[1,3]oxazole]-2′-amine (rac-**25**).* To a solution of 3-bromo-7-hydroxy-spiro[chromeno[2,3-*b*]pyridine]-5,4′-[1,3]oxazole]-2′-amine (650 mg, 1867 μmol) and DMF (7468 μL, 1867 μmol) in a microwave vial were added cesium carbonate (1521 mg, 4668 μmol) and 1-iodo-2,2-dimethylpropane (0.495 mL, 3.74 mmol). The mixture was heated in a microwave at 100 °C for 1 h. An additional portion of 1-iodo-2,2-dimethylpropane (0.4 mL) was added, and the mixture was heated in the microwave at 100 °C for another 1 h. The reaction was diluted with water (5 mL) and EtOAc (5 mL) and stirred for 5 min until homogeneous. The resulting mixture was poured into 10 mL of ethyl acetate and 25 mL of saturated ammonium chloride, and the layers were separated. The aqueous layer was extracted with ethyl acetate (3 × 20 mL). The aqueous layer was then extracted with DCM (3 × 15 mL). The organic layers were each washed with brine, combined, dried over sodium sulfate, filtered, and concentrated. The resulting oil was purified by silica gel chromatography (0−100% EtOAc/hexanes) to provide 3-bromo-7-(2,2-dimethylpropoxy)-spiro-[chromeno[2,3-*b*]pyridine]-5,4′-[1,3]oxazole]-2′-amine (375 mg, 48% yield) as a yellow solid. MS *m*/*z* = 418.2 [M + H]$^+$. Calcd for $C_{19}H_{21}BrN_3O_3$: 418.1.

*(S)-3-(Neopentyloxy)-7-(pyrimidin-5-yl)-5′H-spiro[chromeno[2,3-b]pyridine-5,4′-oxazol]-2′-amine (**26**).* A sealable tube was charged with (*S*)-7-bromo-3-(neopentyloxy)-5′*H*-spiro[chromeno[2,3-*b*]-pyridine-5,4′-oxazol]-2′-amine (75 mg, 0.179 mmol), pyrimidin-5-ylboronic acid (89 mg, 0.717 mmol), potassium carbonate (124 mg, 0.897 mmol), $PdCl_2(AmPhos)_2$ (6.35 mg, 8.97 μmol), THF (1793 μL), and water (1 mL). The tube was flushed with Ar(g), sealed, and heated to 110 °C for 1 h. The reaction was diluted with water (25 mL) and poured into a separatory funnel containing ethyl acetate (25 mL). The layers were separated, and the aqueous layer was extracted with ethyl acetate (2 × 10 mL). The combined organic layers were washed with brine, dried over sodium sulfate, filtered, and concentrated in vacuo to provide a brown foam. This residue was purified by silica gel chromatography (0−10% MeOH/DCM with 0.1% ammonium hydroxide) to provide a tan solid. This solid was purified further by chromatography on silica gel (0−100% EtOAc/DCM) to provide (*S*)-3-(neopentyloxy)-7-(pyrimidin-5-yl)-5′*H*-spiro[chromeno[2,3-*b*]-pyridine-5,4′-oxazol]-2′-amine (54 mg, 0.129 mmol, 72.1% yield) as a light-yellow solid. ^{1}H NMR (400 MHz, DMSO-d_6) δ = 9.19 (s, 1 H),

dx.doi.org/10.1021/jm5012676 | J. Med. Chem. XXXX, XXX, XXX−XXX

9.10 (s, 2 H), 8.01 (d, J = 2.9 Hz, 1 H), 7.79 (dd, J = 2.3, 8.5 Hz, 1 H), 7.67 (d, J = 2.2 Hz, 1 H), 7.36 (d, J = 8.5 Hz, 1 H), 7.30 (d, J = 3.0 Hz, 1 H), 6.51 (br s, 2 H), 4.32 (s, 2 H), 3.79−3.65 (m, 2 H), 1.02 (s, 9 H). MS m/z = 418.2 $[M + H]^+$. Calcd for $C_{23}H_{24}N_5O_3$: 418.2.

*(S)-3-(Neopentyloxy)-7-(pyridin-3-yl)-5′H-spiro[chromeno[2,3-b]-pyridine-5,4′-oxazol]-2′-amine (**27**).* A sealable tube was charged with (*S*)-7-bromo-3-(neopentyloxy)-5′*H*-spiro[chromeno[2,3-*b*]pyridine-5,4′-oxazol]-2′-amine (150 mg, 0.359 mmol), 3-pyridylboronic acid (132 mg, 1.076 mmol), potassium carbonate (248 mg, 1.793 mmol), tetrakis(triphenylphosphine)palladium(0) (20.72 mg, 0.018 mmol), THF (3586 μL), and water (0.5 mL). The tube was flushed with Ar(g), sealed, and heated to 110 °C for 1 h. The reaction was diluted with water (25 mL) and poured into a separatory funnel containing ethyl acetate (50 mL). The layers were separated, and the aqueous layer was extracted with ethyl acetate (2 × 10 mL). The combined organic layers were washed with brine, dried over sodium sulfate, filtered, and concentrated in vacuo to provide a brown foam. This residue was purified by silica gel chromatography (0−10% MeOH/DCM with 0.1% ammonium hydroxide) to provide (*S*)-3-(neopentyloxy)-7-(pyridin-3-yl)-5′*H*-spiro[chromeno[2,3-*b*]pyridine-5,4′-oxazol]-2′-amine (116 mg, 0.279 mmol, 78% yield) as a light-yellow foam. ^{1}H NMR (400 MHz, DMSO-d_6) δ = 8.85 (d, J = 1.9 Hz, 1 H), 8.57 (dd, J = 1.6, 4.8 Hz, 1 H), 8.06−7.95 (m, 2 H), 7.71 (dd, J = 2.3, 8.5 Hz, 1 H), 7.58 (d, J = 2.2 Hz, 1 H), 7.50 (dd, J = 4.8, 7.9 Hz, 1 H), 7.35−7.29 (m, 2 H), 6.52 (s, 2 H), 4.35−4.22 (m, 2 H), 3.77−3.65 (m, 2 H), 1.02 (s, 9 H). MS m/z = 417.2 $[M + H]^+$. Calcd for $C_{24}H_{25}N_4O_3$: 417.2.

*(S)-7-(2-Fluoropyridin-3-yl)-3-(neopentyloxy)-5′H-spiro-[chromeno[2,3-b]pyridine-5,4′-oxazol]-2′-amine (**28**).* A sealable tube was charged with (*S*)-7-bromo-3-(neopentyloxy)-5′*H*-spiro-[chromeno[2,3-*b*]pyridine-5,4′-oxazol]-2′-amine (104822−28) (75 mg, 0.179 mmol), 2-fluoropyridin-3-ylboronic acid (76 mg, 0.538 mmol), potassium carbonate (124 mg, 0.897 mmol), $PdCl_2(AmPhos)_2$ (6.35 mg, 8.97 μmol), THF (1793 μL), and water (1 mL). The tube was flushed with Ar(g), sealed, and heated to 110 °C for 1 h. The reaction was diluted with water (25 mL) and poured into a separatory funnel containing ethyl acetate (25 mL). The layers were separated, and the aqueous layer was extracted with ethyl acetate (2 × 10 mL). The combined organic layers were washed with brine, dried over sodium sulfate, filtered, and concentrated in vacuo to provide a brown foam. This residue was purified by silica gel chromatography (0−10% MeOH/DCM with 0.1% ammonium hydroxide) to provide (*S*)-7-(2-fluoropyridin-3-yl)-3-(neopentyloxy)-5′*H*-spiro[chromeno[2,3-*b*]-pyridine-5,4′-oxazol]-2′-amine (70 mg, 0.161 mmol, 90% yield) as a light-yellow solid. ^{1}H NMR (400 MHz, DMSO-d_6) δ = 8.24 (d, J = 4.7 Hz, 1 H), 8.15−8.07 (m, 1 H), 8.00 (d, J = 3.0 Hz, 1 H), 7.61 (d, J = 8.9 Hz, 1 H), 7.54 (s, 1 H), 7.49 (ddd, J = 1.9, 5.0, 7.2 Hz, 1 H), 7.35−7.27 (m, 2 H), 6.53 (s, 2 H), 4.30−4.20 (m, 2 H), 3.78−3.66 (m, 2 H), 1.02 (s, 9 H). MS m/z = 435.0 $[M + H]^+$. Calcd for $C_{24}H_{24}FN_4O_3$: 435.1.

*(S)-7-(2,2-Dimethylpropoxy)-3-(5-pyrimidinyl)-spiro[chromeno-[2,3-b]pyridine]-5,4′-[1,3]oxazole]-2′-amine (**29**).* A sealable tube was charged with 3-bromo-7-(2,2-dimethylpropoxy)-spiro[chromeno[2,3-*b*]pyridine]-5,4′-[1,3]oxazole]-2′-amine (0.120 g, 287 μmol), pyrimidin-5-ylboronic acid (98 mg, 789 μmol), $Pd(Ph_3P)_4$ (33 mg, 29 μmol), THF (8 mL), and an aqueous solution of potassium carbonate (1 M) (1434 μL, 1434 μmol). The tube was sealed and heated at 90 °C for 2.5 h. The reaction was cooled to room temperature and diluted with water (15 mL). The organics were removed, and the aqueous layer was extracted with ethyl acetate (3 × 45 mL). The combined organics were washed with brine, dried over sodium sulfate, filtered, and concentrated to provide a residue which was purified by chromatography on silica gel (0−10% MeOH/DCM) to provide *rac*-7-(2,2-dimethylpropoxy)-3-(5-pyrimidinyl)-spiro[chromeno[2,3-*b*]pyridine]-5,4′-[1,3]oxazole]-2′-amine as a yellow solid. MS m/z = 418.2 $[M + H]^+$. Calcd for $C_{23}H_{24}N_5O_3$: 418.2. Chiral separation of racemic 7-(2,2-dimethylpropoxy)-3-(5-pyrimidinyl)-spiro[chromeno[2,3-*b*]-pyridine]-5,4′-[1,3]oxazole]-2′-amine: Racemic 7-(2,2-dimethylpropoxy)-3-(5-pyrimidinyl)-spiro[chromeno[2,3-*b*]pyridine]-5,4′-[1,3]-oxazole]-2′-amine (69 mg) was subjected to SFC using 15:85:0.1 MeOH:CO_2:DEA at 70 mL/min on a 2 cm × 15 cm, 5 μm ChiralPak AD-H column and 100 bar system pressure. The first peak (RT = 3.2 min) provided (*S*)-7-(2,2-dimethylpropoxy)-3-(5-pyrimidinyl)-spiro-[chromeno[2,3-*b*]pyridine]-5,4′-[1,3]oxazole]-2′-amine (29 mg, 24% yield, >99% ee), and the second peak (RT = 6.8 min) provided (*R*)-7-(2,2-dimethylpropoxy)-3-(5-pyrimidinyl)-spiro[chromeno[2,3-*b*]-pyridine]-5,4′-[1,3]oxazole]-2′-amine (>99% ee). ^{1}H NMR (400 MHz, DMSO-d_6) δ = 9.22 (s, 1 H), 9.18 (s, 2 H), 8.69 (d, J = 2.4 Hz, 1 H), 8.15 (d, J = 2.4 Hz, 1 H), 7.19 (d, J = 8.9 Hz, 1 H), 6.98 (dd, J = 3.0, 8.9 Hz, 1 H), 6.81 (d, J = 2.9 Hz, 1 H), 6.52 (s, 2 H), 4.35−4.22 (m, 2 H), 3.62 (q, J = 8.6 Hz, 2 H), 1.01 (s, 9 H).

*(S)-7-(2-Fluoropyridin-3-yl)-3-(2-methoxy-2-methylpropoxy)-5′H-spiro[chromeno[2,3-b]pyridine-5,4′-oxazol]-2′-amine (**30**).* A vial was charged with 2-fluoropyridin-3-ylboronic acid (0.156 g, 1.105 mmol), tetrakis(triphenylphosphine)palladium(0) (0.043 g, 0.037 mmol), potassium carbonate (0.255 g, 1.842 mmol), *rac*-7-bromo-3-(2-methoxy-2-methylpropoxy)-5′*H*-spiro[chromeno[2,3-*b*]pyridine-5,4′-oxazol]-2′-amine (0.160 g, 0.368 mmol), THF (3 mL), and water (0.5 mL). The resulting mixture was heated to 110 °C for 2 h. The reaction mixture was cooled to room temperature and extracted with EtOAc. The organic layer was dried over $MgSO_4$, filtered, and concentrated. The residue was purified by chromatography on silica gel (0−10% MeOH/DCM) to give *rac*-7-(2-fluoropyridin-3-yl)-3-(2-methoxy-2-methylpropoxy)-5′*H*-spiro[chromeno[2,3-*b*]pyridine-5,4′-oxazol]-2′-amine (0.072 g, 0.160 mmol, 43.4% yield). This material was dissolved in methanol, and the resulting solution was purified by SFC, using 1.5 mL injections on a 5 μm, 3 cm × 15 cm Chiralpak IC column with 40% MeOH/0.2% diethylamine/60% CO_2 at a flow rate of 100 mL/min. This afforded peak 1, (*S*)-7-(2-fluoropyridin-3-yl)-3-(2-methoxy-2-methylpropoxy)-5′*H*-spiro[chromeno[2,3-*b*]pyridine-5,4′-oxazol]-2′-amine (0.026 g, 0.058 mmol, 15.67% yield), and peak 2, (*R*)-7-(2-fluoropyridin-3-yl)-3-(2-methoxy-2-methylpropoxy)-5′*H*-spiro[chromeno[2,3-*b*]pyridine-5,4′-oxazol]-2′-amine (0.026 g, 0.058 mmol, 15.67% yield). Data for the title compound. ^{1}H NMR (400 MHz, acetonitrile-d_3) δ = 8.18 (td, J = 1.6, 4.8 Hz, 1 H), 8.00 (ddd, J = 1.9, 7.5, 10.2 Hz, 1 H), 7.96 (d, J = 2.9 Hz, 1 H), 7.60−7.58 (m, 1 H), 7.57−7.55 (m, 1 H), 7.41−7.35 (m, 2 H), 7.28 (dd, J = 0.7, 8.2 Hz, 1 H), 5.08 (br s, 2 H), 4.32 (d, J = 1.8 Hz, 2 H), 3.93 (d, J = 1.0 Hz, 2 H), 3.23 (s, 3 H), 1.27 (s, 6 H). MS m/z = 451.2 $[M + H]^+$. Calcd for $C_{24}H_{24}FN_4O_4$: 451.2.

*(S)-3-(3,6-Dihydro-2H-pyran-4-yl)-7-(2-fluoropyridin-3-yl)-5′H-spiro[chromeno[2,3-b]pyridine-5,4′-oxazol]-2′-amine (**31**).* A vial was charged with (*S*)-3-bromo-7-(2-fluoropyridin-3-yl)-5′*H*-spiro-[chromeno[2,3-*b*]pyridine-5,4′-oxazol]-2′-amine (0.150 g, 0.351 mmol), $Pd(Ph_3P)_4$ (0.020 g, 0.018 mmol), potassium carbonate (0.243 g, 1.756 mmol), 1,4-dioxane (1.756 mL), and water (0.585 mL). The vial was flushed with argon, sealed, and heated overnight at 80 °C. The mixture was cooled to room temperature and then diluted water and extracted with ethyl acetate (2×). The combined organic extracts were dried with sodium sulfate, filtered, and concentrated. The residue was purified by chromatography on silica gel (0−6% MeOH/DCM0 to afford (*S*)-3-(3,6-dihydro-2*H*-pyran-4-yl)-7-(2-fluoropyridin-3-yl)-5′*H*-spiro[chromeno[2,3-*b*]pyridine-5,4′-oxazol]-2′-amine (0.089 g, 0.207 mmol, 58.9% yield) as a white solid. ^{1}H NMR (400 MHz, DMSO-d_6) δ = 8.39 (d, J = 2.4 Hz, 1 H), 8.25 (td, J = 1.5, 4.9 Hz, 1 H), 8.12 (ddd, J = 1.9, 7.5, 10.3 Hz, 1 H), 7.79 (d, J = 2.4 Hz, 1 H), 7.62 (td, J = 1.9, 8.5 Hz, 1 H), 7.56 (t, J = 1.8 Hz, 1 H), 7.49 (ddd, J = 1.9, 5.0, 7.3 Hz, 1 H), 7.37 (d, J = 8.5 Hz, 1 H), 6.51 (s, 2 H), 6.31 (t, J = 1.5 Hz, 1 H), 4.28 (s, 2 H), 4.25 (q, J = 2.6 Hz, 2 H), 3.85 (t, J = 5.5 Hz, 2 H). MS m/z = 431.1 $[M + H]^+$. Calcd for $C_{24}H_{20}FN_4O_3$: 431.1.

*(S)-3-(5,6-Dihydro-2H-pyran-3-yl)-7-(2-fluoropyridin-3-yl)-5′H-spiro[chromeno[2,3-b]pyridine-5,4′-oxazol]-2′-amine (**32**).* A vial was charged with (*S*)-3-bromo-7-(2-fluoropyridin-3-yl)-5′*H*-spiro-[chromeno[2,3-*b*]pyridine-5,4′-oxazol]-2′-amine (129 mg, 0.302 mmol), 2-(5,6-dihydro-2*H*-pyran-3-yl)-4,4,5,5-tetramethyl-1,3,2-dioxaborolane (307 mg, 0.453 mmol), potassium carbonate (209 mg, 1.510 mmol), and $PdCl_2(dppf)-CH_2Cl_2$ (12.33 mg, 0.015 mmol). The vial was flushed with Ar(g), and then 1,4-dioxane (1510 μL) and water (0.5 mL) were added in sequence. The vial was sealed and heated to

dx.doi.org/10.1021/jm5012676 | J. Med. Chem. XXXX, XXX, XXX−XXX

70 °C for 40 min. The mixture was diltued with EtOAc (15 mL) and water (15 mL). The layers were separated, and the aqueous layer was extracted with EtOAc (15 mL). The combined organic extracts were dried over sodium sulfate, filtered, and evaporated. The residue was purified by chromatography on silica gel (0−50% of a 90:10:1 mix of DCM/MeOH/NH_4OH in DCM) to give ca. 60 mg of a brown solid. The solid was dissolved in MeOH, and the resulting solution was loaded onto a 2-g SCX acidic ion exchange column. The column was eluted with MeOH, then with 2N ammonia in methanol. The basic fraction was concentrated to give (*S*)-3-(5,6-dihydro-2*H*-pyran-3-yl)-7-(2-fluoropyridin-3-yl)-5′*H*-spiro[chromeno[2,3-*b*]pyridine-5,4′-oxazol]-2′-amine (52.48 mg, 0.122 mmol, 40.4% yield) as an off-white solid. ^{1}H NMR (400 MHz, DMSO-d_6) δ = 8.30 (d, *J* = 2.4 Hz, 1 H), 8.25 (td, *J* = 1.5, 4.8 Hz, 1 H), 8.11 (ddd, *J* = 2.0, 7.5, 10.3 Hz, 1 H), 7.73 (d, *J* = 2.4 Hz, 1 H), 7.62 (td, *J* = 1.7, 8.8 Hz, 1 H), 7.56 (t, *J* = 1.8 Hz, 1 H), 7.49 (ddd, *J* = 1.9, 5.0, 7.2 Hz, 1 H), 7.36 (d, *J* = 8.5 Hz, 1 H), 6.53 (br s, 2 H), 6.32 (td, *J* = 2.2, 3.9 Hz, 1 H), 4.45 (qd, *J* = 2.3, 6.6 Hz, 2 H), 4.28 (s, 2 H), 3.76 (t, *J* = 5.5 Hz, 2 H), 2.28 (qd, *J* = 2.7, 6.8 Hz, 2 H). MS *m*/*z* = 431.0 [M + H]$^+$. Calcd for $C_{24}H_{20}FN_4O_3$: 431.1.

*(S)-7-(2-Fluoropyridin-3-yl)-3-(tetrahydro-2H-pyran-4-yl)-5′H-spiro[chromeno[2,3-b]pyridine-5,4′-oxazol]-2′-amine (**33**).* A vial was charged with (*S*)-2′-amino-3-(tetrahydro-2*H*-pyran-4-yl)-5′*H*-spiro[chromeno[2,3-*b*]pyridine-5,4′-oxazole]-7-yl trifluoromethanesulfonate (70.0 mg, 0.144 mmol), 2-fluoropyridin-3-ylboronic acid (61.0 mg, 0.433 mmol), potassium carbonate (100 mg, 0.721 mmol), and $Pd(Ph_3P)_4$ (8.33 mg, 7.21 μmol). The vial was flushed with Ar(g), and then 1,4-dioxane (721 μL) and water (0.3 mL) were added in sequence. The vial was sealed and heated to 80 °C for 50 min. The mixture was diluted with brine (20 mL) and extracted with EtOAc (2 × 15 mL). The combined organic extracts were dried over sodium sulfate, filtered, and evaporated. The residue was purified by chromatography on silica gel (0−70% of a 90:10:1 mix of DCM/MeOH/NH_4OH in DCM) to give (*S*)-7-(2-fluoropyridin-3-yl)-3-(tetrahydro-2*H*-pyran-4-yl)-5′*H*-spiro[chromeno[2,3-*b*]pyridine-5,4′-oxazol]-2′-amine (60.4 mg, 0.140 mmol, 97% yield) as a white solid. ^{1}H NMR (400 MHz, DMSO-d_6) δ = 8.24 (d, *J* = 4.8 Hz, 1 H), 8.20 (d, *J* = 2.2 Hz, 1 H), 8.11 (ddd, *J* = 1.9, 7.7, 10.1 Hz, 1 H), 7.66 (d, *J* = 2.2 Hz, 1 H), 7.61 (d, *J* = 8.6 Hz, 1 H), 7.56 (s, 1 H), 7.49 (ddd, *J* = 1.8, 5.0, 7.2 Hz, 1 H), 7.35 (d, *J* = 8.5 Hz, 1 H), 6.51 (s, 2 H), 4.28−4.21 (m, 2 H), 4.00−3.93 (m, 2 H), 3.50−3.39 (m, 2 H), 2.95−2.84 (m, 1 H), 1.79−1.60 (m, 4 H). MS *m*/*z* = 433.0 [M + H]$^+$. Calcd for $C_{24}H_{22}FN_4O_3$: 433.2.

*(S)-3-(6,6-Dimethyl-3,6-dihydro-2H-pyran-4-yl)-7-(2-fluoropyridin-3-yl)-5′H-spiro[chromeno[2,3-b]pyridine-5,4′-oxazol]-2′-amine (**34**).* A vial was charged with (*S*)-2′-amino-3-(6,6-dimethyl-3,6-dihydro-2*H*-pyran-4-yl)-5′*H*-spiro[chromeno[2,3-*b*]pyridine-5,4′-oxazole]-7-yl trifluoromethanesulfonate (0.130 g, 0.254 mmol), 2-fluoropyridin-3-ylboronic acid (0.107 g, 0.763 mmol), and $Pd(Ph_3P)_4$ (0.015 g, 0.013 mmol). The vial was purged with Ar(g), and then DMF (1.271 mL) and potassium carbonate (0.635 mL, 1.271 mmol) (as a 2.0 M aq solution) were added in sequence. The vial was sealed and stirred at 70 °C overnight. In the morning, the reaction was diluted with ethyl acetate and washed with water. The aqueous layer was extracted with ethyl acetate, and the combined organic layers were dried with sodium sulfate, filtered, and concentrated. The material was purified via chromatography on silica gel (0−5% MeOH/DCM) afford 30 mg of product as an off-white solid. The impure fractions were combined and repurified via chromatography on silica gel (0−5% MeOH/DCM). Fractions containing clean desired product were combined with the previously isolated material and concentrated to afford (*S*)-3-(6,6-dimethyl-3,6-dihydro-2*H*-pyran-4-yl)-7-(2-fluoropyridin-3-yl)-5′*H*-spiro[chromeno[2,3-*b*]pyridine-5,4′-oxazol]-2′-amine (0.044 g, 0.096 mmol, 37.8% yield) as a white solid. ^{1}H NMR (400 MHz, DMSO-d_6) δ = 8.37 (d, *J* = 2.4 Hz, 1 H), 8.25 (td, *J* = 1.5, 4.8 Hz, 1 H), 8.11 (ddd, *J* = 1.9, 7.5, 10.3 Hz, 1 H), 7.78 (d, *J* = 2.5 Hz, 1 H), 7.62 (td, *J* = 1.7, 8.8 Hz, 1 H), 7.56 (t, *J* = 1.8 Hz, 1 H), 7.49 (ddd, *J* = 2.0, 5.0, 7.3 Hz, 1 H), 7.36 (d, *J* = 8.5 Hz, 1 H), 6.52 (s, 2 H), 6.22 (t, *J* = 1.4 Hz, 1 H), 4.28 (s, 2 H), 3.84 (t, *J* = 5.4 Hz, 2 H), 2.41−2.35 (m, 2 H), 1.28 (s, 6 H). MS *m*/*z* = 459.3 [M + H]$^+$. Calcd for $C_{26}H_{24}FN_4O_3$: 459.2.

*(S)-7-(2-Fluoropyridin-3-yl)-3-morpholino-5′H-spiro[chromeno-[2,3-b]pyridine-5,4′-oxazol]-2′-amine (**35**).* A vial was charged (*S*)-2′-amino-3-morpholino-5′*H*-spiro[chromeno[2,3-*b*]pyridine-5,4′-oxazole]-7-yl trifluoromethanesulfonate (0.060 g, 0.123 mmol), 2-fluoropyridin-3-ylboronic acid (0.052 g, 0.370 mmol), potassium carbonate (0.085 g, 0.617 mmol), and $Pd(Ph_3P)_4$ (7.13 mg, 6.17 μmol). The vial was flushed with Ar(g) and then 1,4-dioxane (0.617 mL) and water (0.36 mL). The vial was sealed and heated at 75 °C for 1 h. The reaction mixture was diluted with ethyl acetate and washed with water. The aqueous layer was extracted with ethyl acetate, and the combined organic extracts were washed with brine, dried over sodium sulfate, filtered, and concentrated. The material was purified via chromatography on silica gel (0−10% MeOH/DCM) to give partially purified material. This material was purified further by reverse-phase HPLC (20−90% CH_3CN/H_2O with 0.1% TFA). Fractions containing clean desired product were combined, and the combined solution was partitioned between DCM and saturated aq sodium bicarbonate solution. The aqueous layer was extracted with DCM, and the combined organic extracts were dried with sodium sulfate, filtered, and concentrated to afford (*S*)-7-(2-fluoropyridin-3-yl)-3-morpholino-5′*H*-spiro[chromeno[2,3-*b*]pyridine-5,4′-oxazol]-2′-amine (0.018 g, 0.042 mmol, 33.7% yield) as a white solid. ^{1}H NMR (400 MHz, DMSO-d_6) δ = 8.24 (td, *J* = 1.6, 4.8 Hz, 1 H), 8.10 (ddd, *J* = 1.9, 7.5, 10.4 Hz, 1 H), 8.00 (d, *J* = 2.9 Hz, 1 H), 7.60 (td, *J* = 1.7, 8.8 Hz, 1 H), 7.53 (t, *J* = 1.8 Hz, 1 H), 7.49 (ddd, *J* = 1.9, 5.0, 7.3 Hz, 1 H), 7.35−7.28 (m, 2 H), 6.50 (s, 2 H), 4.24 (s, 2 H), 3.77 (t, *J* = 4.8 Hz, 4 H), 3.16−3.08 (m, 4 H). MS *m*/*z* = 434.4 [M + H]$^+$. Calcd for $C_{23}H_{21}FN_5O_3$: 434.2.

*(S)-7-(2-Fluoropyridin-3-yl)-3-(p-tolyl)-5′H-spiro[chromeno[2,3-b]pyridine-5,4′-oxazol]-2′-amine (**36**).* A vial was charged with (*S*)-2′-amino-3-*p*-tolyl-5′*H*-spiro[chromeno[2,3-*b*]pyridine-5,4′-oxazole]-7-yl trifluoromethanesulfonate (45.0 mg, 0.092 mmol), 2-fluoropyridin-3-ylboronic acid (38.7 mg, 0.275 mmol), potassium carbonate (229 μL, 0.458 mmol), and $Pd(Ph_3P)_4$ (5.29 mg, 4.58 μmol). The vial was flushed with Ar(g), and then 1,4-dioxane (1 mL) and water (0.5 mL) were added in sequence. The vial was sealed and heated to 80 °C for 1 h. The mixture was diluted with EtOAc, washed with brine, dried over sodium sulfate, filtered, and evaporated. The residue was purified by chromatography on silica gel (0−5% MeOH/DCM) to give (*S*)-7-(2-fluoropyridin-3-yl)-3-*p*-tolyl-5′*H*-spiro[chromeno[2,3-*b*]pyridine-5,4′-oxazol]-2′-amine (29.53 mg, 0.067 mmol, 73.6% yield) as a tan solid. ^{1}H NMR (400 MHz, DMSO-d_6) δ = 8.57 (d, *J* = 2.4 Hz, 1 H), 8.25 (td, *J* = 1.6, 4.8 Hz, 1 H), 8.13 (ddd, *J* = 1.9, 7.5, 10.3 Hz, 1 H), 7.97 (d, *J* = 2.4 Hz, 1 H), 7.67−7.56 (m, 4 H), 7.50 (ddd, *J* = 1.9, 5.0, 7.3 Hz, 1 H), 7.39 (d, *J* = 8.5 Hz, 1 H), 7.33 (d, *J* = 7.8 Hz, 2 H), 6.54 (s, 2 H), 4.41−4.25 (m, 2 H), 2.36 (s, 3 H). MS *m*/*z* = 439.0 [M + H]$^+$. Calcd for $C_{26}H_{20}FN_4O_2$: 439.2.

*(SS)-4-(2′-Amino-7-(2-fluoropyridin-3-yl)-5′H-spiro[chromeno-[2,3-b]pyridine-5,4′-oxazol]-3-yl)benzonitrile (**37**).* A vial was charged with (*S*)-2′-amino-3-(4-cyanophenyl)-5′*H*-spiro[chromeno[2,3-*b*]-pyridine-5,4′-oxazole]-7-yl trifluoromethanesulfonate (50 mg, 0.100 mmol), 2-fluoropyridin-3-ylboronic acid (42.1 mg, 0.299 mmol), potassium carbonate (68.8 mg, 0.498 mmol), and $Pd(Ph_3P)_4$ (5.75 mg, 4.98 μmol). The vial was flushed with Ar(g), and then 1,4-dioxane (498 μL) and water (0.25 mL) were added in sequence. The vial was sealed and heated to 80 °C for 2.5 h. The mixture was diluted with EtOAc (20 mL), washed with water (15 mL), dried over sodium sulfate, filtered, and evaporated. The residue was purified by chromatography on silica gel (0−100% of a 90:10:1 mix of DCM/MeOH/NH_4OH in DCM) to give (*S*)-4-(2′-amino-7-(2-fluoropyridin-3-yl)-5′*H*-spiro[chromeno[2,3-*b*]pyridine-5,4′-oxazole]-3-yl)-benzonitrile (35.91 mg, 0.080 mmol, 80% yield) as a white solid. ^{1}H NMR (400 MHz, DMSO-d_6) δ = 8.70 (d, *J* = 2.4 Hz, 1 H), 8.28−8.23 (m, 1 H), 8.17−8.07 (m, 2 H), 8.02−7.89 (m, 4 H), 7.67−7.62 (m, 1 H), 7.58 (t, *J* = 1.8 Hz, 1 H), 7.50 (ddd, *J* = 2.0, 4.9, 7.4 Hz, 1 H), 7.41 (d, *J* = 8.5 Hz, 1 H), 6.54 (s, 2 H), 4.45−4.26 (m, 2 H). MS *m*/*z* = 450.0 [M + H]$^+$. Calcd for $C_{26}H_{17}FN_5O_2$: 450.1.

*(S)-7-(2-Fluoropyridin-3-yl)-3-(2-fluoropyridin-4-yl)-5′H-spiro-[chromeno[2,3-b]pyridine-5,4′-oxazol]-2′-amine (**38**).* A vial was

dx.doi.org/10.1021/jm5012676 | J. Med. Chem. XXXX, XXX, XXX−XXX

charged with (*S*)-3-bromo-7-(2-fluoropyridin-3-yl)-5′*H*-spiro-[chromeno[2,3-*b*]pyridine-5,4′-oxazol]-2′-amine (70 mg, 0.164 mmol), 2-fluoropyridin-4-ylboronic acid (69.3 mg, 0.492 mmol), potassium carbonate (113 mg, 0.819 mmol), and $Pd(Ph_3P)_4$ (9.47 mg, 8.19 μmol). The vial was flushed with Ar(g), and then 1,4-dioxane (819 μL) and water (1 mL) were added in sequence. The vial was sealed and heated to 80 °C for 3 h. The mixture was cooled and diluted with EtOAc (15 mL) and brine (15 mL). The layers were separated, and the aqueous layer was extracted with EtOAc (15 mL). The combined organic extracts were dried over sodium sulfate, filtered, and evaporated. The residue was purified by chromatography on silica gel (0−70% of a 90:10:1 mix of DCM/MeOH/NH_4OH in DCM) to afford (*S*)-7-(2-fluoropyridin-3-yl)-3-(2-fluoropyridin-4-yl)-5′*H*-spiro-[chromeno[2,3-*b*]pyridine-5,4′-oxazol]-2′-amine (31.26 mg, 0.070 mmol, 43.0% yield) as a white solid. ^{1}H NMR (400 MHz, DMSO-d_6) δ = 8.81 (d, *J* = 2.4 Hz, 1 H), 8.36 (d, *J* = 5.4 Hz, 1 H), 8.26 (td, *J* = 1.5, 4.8 Hz, 1 H), 8.23 (d, *J* = 2.4 Hz, 1 H), 8.16−8.10 (m, 1 H), 7.76 (td, *J* = 1.8, 5.3 Hz, 1 H), 7.68−7.63 (m, 2 H), 7.57 (t, *J* = 1.8 Hz, 1 H), 7.50 (ddd, *J* = 1.9, 5.0, 7.3 Hz, 1 H), 7.42 (d, *J* = 8.5 Hz, 1 H), 6.52 (s, 2 H), 4.45−4.41 (m, 1 H), 4.39−4.36 (m, 1 H). MS *m*/*z* = 444.0 [M + H]$^+$. Calcd for $C_{24}H_{16}F_2N_5O_2$: 444.1.

*(S)-3-(3,3-Dimethylbut-1-yn-1-yl)-7-(2-fluoropyridin-3-yl)-5′H-spiro[chromeno[2,3-b]pyridine-5,4′-oxazol]-2′-amine (**39**).* A vial was charged with (*S*)-3-bromo-7-(2-fluoropyridin-3-yl)-5′*H*-spiro-[chromeno[2,3-*b*]pyridine-5,4′-oxazol]-2′-amine (80 mg, 0.187 mmol), $Pd(Ph_3P)_4$ (21.64 mg, 0.019 mmol), CuI (3.57 mg, 0.019 mmol), THF (0.75 mL), and DMF (0.75 mL). *N*,*N*-Diisopropylamine (525 μL, 3.75 mmol) and 3,3-dimethylbut-1-yne (115 μL, 0.936 mmol) were added in sequence. The vial was flushed with Ar(g), sealed, and heated to 110 °C for 3 h. The mixture was partitioned between water (10 mL) and EtOAc (10 mL). The layers were separated, and the aqueous layer was extracted with EtOAc (2 × 10 mL). The combined organic extracts were dried over sodium sulfate, filtered, and evaporated. The residue was purified by chromatography on silica gel (0−70% of a 90:10:1 mixture of DCM/MeOH/NH_4OH in DCM) to give 80 mg of a solid. This solid was dissolved in MeOH and purified further by reverse-phase HPLC (10−90% CH_3CN/H_2O with 0.1% TFA). The fractions containing product were combined in saturated aq sodium bicarbonate solution with the aid of methanol and extracted with DCM (3×). The combined organic extracts were dried over sodium sulfate, filtered, and evaporated to give (*S*)-3-(3,3-dimethylbut-1-ynyl)-7-(2-fluoropyridin-3-yl)-5′*H*-spiro[chromeno-[2,3-*b*]pyridine-5,4′-oxazol]-2′-amine (46.61 mg, 0.109 mmol, 58.1% yield) as a white powder. ^{1}H NMR (500 MHz, DMSO-d_6) δ = 8.27 (d, *J* = 2.2 Hz, 1 H), 8.25 (td, *J* = 1.4, 4.8 Hz, 1 H), 8.12 (ddd, *J* = 1.9, 7.5, 10.3 Hz, 1 H), 7.67 (d, *J* = 2.3 Hz, 1 H), 7.65−7.61 (m, 1 H), 7.58−7.56 (m, 1 H), 7.49 (ddd, *J* = 1.8, 5.0, 7.2 Hz, 1 H), 7.36 (d, *J* = 8.5 Hz, 1 H), 6.55 (s, 2 H), 4.30−4.27 (m, 1 H), 4.25−4.22 (m, 1 H), 1.32 (s, 9 H). MS *m*/*z* = 429.0 [M + H]$^+$. Calcd for $C_{25}H_{22}FN_4O_2$: 429.2.

*(S)-7-(2-Fluoropyridin-3-yl)-3-(3-methoxy-3-methylbut-1-yn-1-yl)-5′H-spiro[chromeno[2,3-b]pyridine-5,4′-oxazol]-2′-amine (**40**).* A vial was charged with (*S*)-3-bromo-7-(2-fluoropyridin-3-yl)-5′*H*-spiro[chromeno[2,3-*b*]pyridine-5,4′-oxazol]-2′-amine (169 mg, 0.396 mmol), CuI (7.53 mg, 0.040 mmol), and $Pd(Ph_3P)_4$ (45.7 mg, 0.040 mmol). DMF (791 μL), *i*-Pr_2NH (0.8 mL), and 3-methoxy-3-methylbut-1-yne (143 μL, 1.187 mmol) were added in sequence, and the vial was sealed and heated to 90 °C for 3.5 h. The reaction mixture was diluted with water and extracted with EtOAc (2×). The combined organic extracts were dried over sodium sulfate, filtered, and concentrated under vacuum. The residue was purified by chromatography on silica gel (0−100% of a 90:10:1 mix of DCM/MeOH/NH_4OH in DCM) to give a yellow oil. This oil was dissolved in MeOH and loaded onto a 5-g SCX-2 acidic ion exchange column. The column was eluted with methanol, then with 2N ammonia in methanol. The basic fraction was concentrated under vacuum to give (*S*)-7-(2-fluoropyridin-3-yl)-3-(3-methoxy-3-methylbut-1-ynyl)-5′*H*-spiro[chromeno[2,3-*b*]pyridine-5,4′-oxazol]-2′-amine (167.79 mg, 0.378 mmol, 95% yield) as a white solid. ^{1}H NMR (400 MHz, DMSO-d_6) δ = 8.38 (d, *J* = 2.2 Hz, 1 H), 8.25 (td, *J* = 1.5, 3.3 Hz, 1 H), 8.17−8.08 (m, 1 H), 7.76 (d, *J* = 2.2 Hz, 1 H), 7.64 (td, *J* = 1.7, 8.6 Hz, 1 H), 7.57 (d, *J* = 1.7 Hz, 1 H), 7.49 (ddd, *J* = 1.9, 5.1, 7.3 Hz, 1 H), 7.38 (d, *J* = 8.5 Hz, 1 H), 6.58 (br s, 2 H), 4.34−4.29 (m, 1 H), 4.28−4.22 (m, 1 H), 3.33 (s, 3 H), 1.50 (s, 6 H). MS *m*/*z* = 445.0 [M + H]$^+$. Calcd for $C_{25}H_{22}FN_4O_3$: 445.2.

*(S)-4-(2′-Amino-7-(2-fluoropyridin-3-yl)-5′H-spiro[chromeno[2,3-b]pyridine-5,4′-oxazol]-3-yl)-2-methylbut-3-yn-2-ol (**41**).* A vial was charged with (*S*)-3-bromo-7-(2-fluoropyridin-3-yl)-5′*H*-spiro-[chromeno[2,3-*b*]pyridine-5,4′-oxazol]-2′-amine (101 mg, 0.237 mmol), $Pd(Ph_3P)_4$ (27.4 mg, 0.024 mmol), CuI (4.51 mg, 0.024 mmol), THF (0.95 mL), and DMF (0.95 mL). *N*,*N*-Diisopropylamine (664 μL, 4.74 mmol) and 2-methylbut-3-yn-2-ol (116 μL, 1.184 mmol) were added in sequence. The vial was flushed with Ar(g), sealed, and heated at 110 °C for 2.5 h. The reaction mixture was diluted with water and extracted with EtOAc (3×). The combined organic extracts were dried over sodium sulfate, filtered, and evaporated. The residue was purified by chromatography on silica gel (0−100% of a 90:10:1 mixture of DCM/MeOH/NH_4OH) to give (*S*)-4-(2′-amino-7-(2-fluoropyridin-3-yl)-5′*H*-spiro[chromeno[2,3-*b*]-pyridine-5,4′-oxazol]-3-yl)-2-methylbut-3-yn-2-ol (36.4 mg, 60% yield) as an off-white solid. ^{1}H NMR (400 MHz, DMSO-d_6) δ = 8.31 (d, *J* = 2.2 Hz, 1 H), 8.25 (td, *J* = 1.5, 4.8 Hz, 1 H), 8.12 (ddd, *J* = 2.0, 7.5, 10.4 Hz, 1 H), 7.71 (d, *J* = 2.2 Hz, 1 H), 7.63 (td, *J* = 1.7, 8.8 Hz, 1 H), 7.58 (t, *J* = 1.8 Hz, 1 H), 7.49 (ddd, *J* = 2.0, 5.0, 7.3 Hz, 1 H), 7.37 (d, *J* = 8.5 Hz, 1 H), 6.58 (s, 2 H), 5.54 (s, 1 H), 4.32−4.28 (m, 1 H), 4.23 (d, *J* = 8.7 Hz, 1 H), 1.49 (s, 6 H). MS *m*/*z* = 431.0 [M + H]$^+$. Calcd for $C_{24}H_{20}FN_4O_3$: 431.2.

*Preparation of Trimethyl((3-methyloxetan-3-yl)ethynyl)silane for the Synthesis of **42**.* Step 1: Pyridinium chlorochromate (10.13 g, 47.0 mmol) and silica gel (10 g) were combined and ground with a mortar and pestle until a fine, light-orange powder resulted. The powder was transferred to a 500 mL round-bottom flask and suspended in DCM (157 mL). 3-Methyl-3-oxetanemethanol (3.87 mL, 39.2 mmol) was added in one portion via syringe, and the resulting mixture was stirred for 24 h. The reaction the mixture was filtered through a pad of silica gel, and the filter pad was washed with DCM (2×). The filtrate was carefully evaporated, but not to dryness, to give 5.8193 g of a greenish solution that corresponded to 32 wt % of the 3-methyloxetane-3-carbaldehyde in DCM (as determined by ^{1}H NMR analysis). This solution was used directly in the next reaction. ^{1}H NMR (400 MHz, chloroform-*d*) δ = 9.96 (s, 1 H), 4.88 (d, *J* = 6.3 Hz, 2 H), 4.51 (d, *J* = 6.4 Hz, 2 H), 1.49 (s, 3 H).

Step 2: A 500 mL round-bottom flask was charged with triphenylphosphine (19.51 g, 74.4 mmol) and DCM (93 mL) to give a clear solution. The flask was cooled in an ice bath for 10 min, and then carbon tetrabromide (12.34 g, 37.2 mmol) was added in one portion. After 30 min of stirring, 3-methyloxetane-3-carbaldehyde (5.8193 g, 32 wt % in DCM, 18.60 mmol) was added dropwise to the thick, orange mixture via a pipet (with a 5 mL DCM flask-wash). The resulting mixture was slowly warmed to room temperature over 1 h, then was diluted with hexane (300 mL). The mixture was stirred for 10 min, resulting in the formation of a precipitate. The supernatant was decanted onto a pad of silica gel and filtered. The remaining solid was washed with 10% EtOAc/hexane (3 × 100 mL), each time filtering through the silica gel pad. The combined filtrates were evaporated to give 3-(2,2-dibromovinyl)-3-methyloxetane (3.539 g, 13.83 mmol, 74.3% yield) as a clear oil. ^{1}H NMR (400 MHz, chloroform-*d*) δ = 6.70 (s, 1 H), 4.82 (d, *J* = 5.8 Hz, 2 H), 4.39 (d, *J* = 6.1 Hz, 2 H), 1.61 (s, 3 H).

Step 3: A 250 mL round-bottom flask was charged with 3-(2,2-dibromovinyl)-3-methyloxetane (2.177 g, 8.51 mmol) in THF (85 mL) to give a clear solution. The flask was cooled in a dry ice/acetone bath for 15 min, and then *n*-butyllithium (7.83 mL, 19.56 mmol) (as a 2.5 M solution in hexane) was added dropwise over 5 min. The resulting mixture was stirred for 45 min, and then trimethylchlorosilane (3.81 mL, 29.8 mmol) was added dropwise. The cooling bath was removed, and the mixture was stirred at room temperature for 30 min. The reaction mixture was diluted with water (50 mL) and ether (50 mL). The layers were separated, and the aqueous layer was extracted with ether (25 mL). The combined organic extracts were dried over magnesium sulfate, filtered, and evaporated. The residue

dx.doi.org/10.1021/jm5012676 | J. Med. Chem. XXXX, XXX, XXX−XXX

was dissolved in a small amount of ether and filtered through a silica gel pad. The filtrate was evaporated to give trimethyl((3-methyloxetan-3-yl)ethynyl)silane (1.344 g, 7.99 mmol, 94% yield) as a pale-yellow oil. ^{1}H NMR (400 MHz, DMSO-d_6) δ = 5.75 (s, 1 H), 4.61 (d, J = 5.3 Hz, 2 H), 4.33 (d, J = 5.6 Hz, 3 H), 0.14 (s, 9 H).

*(S)-7-(2-Fluoropyridin-3-yl)-3-((3-methyloxetan-3-yl)ethynyl)-5′H-spiro[chromeno[2,3-b]pyridine-5,4′-oxazol]-2′-amine (**42**).* A round-bottom flask was charged with (*S*)-3-bromo-7-(2-fluoropyridin-3-yl)-5′*H*-spiro[chromeno[2,3-*b*]pyridine-5,4′-oxazol]-2′-amine (5.04 g, 11.80 mmol), copper(i) iodide (0.112 g, 0.590 mmol), $Pd(Ph_3P)_4$ (0.682 g, 0.590 mmol), and tetrabutylammonium fluoride trihydrate (4.63 g, 17.70 mmol). The flask was flushed with Ar(g), and then THF (23.60 mL) and trimethyl((3-methyloxetan-3-yl)ethynyl)-silane (3.35 mL, 17.70 mmol) were added in sequence. The flask was fitted with a reflux condenser and heated to 70 °C for 2 h. The mixture was cooled to room temperature, then poured into a separatory funnel with the aid of EtOAc (25 mL). The organic solution was washed with water (2 × 25 mL), and the aquoeus washes were extracted with EtOAc (25 mL). The organic extracts were combined, and the combined solution was washed with brine (30 mL), dried over sodium sulfate, filtered, and evaporated. The residue was purified by chromatography on silica gel (0−50% of a 90:10:1 mix of DCM/MeOH/NH_4OH in DCM) to give to (*S*)-7-(2-fluoropyridin-3-yl)-3-((3-methyloxetan-3-yl)ethynyl)-5′*H*-spiro[chromeno[2,3-*b*]pyridine-5,4′-oxazol]-2′-amine (4.655 g, 10.52 mmol, 89% yield) as an off-white solid. ^{1}H NMR (400 MHz, DMSO-d_6) δ = 8.36 (d, J = 2.2 Hz, 1 H), 8.25 (td, J = 1.6, 4.8 Hz, 1 H), 8.12 (ddd, J = 1.9, 7.5, 10.4 Hz, 1 H), 7.76 (d, J = 2.2 Hz, 1 H), 7.66−7.61 (m, 1 H), 7.57 (t, J = 1.8 Hz, 1 H), 7.49 (ddd, J = 1.9, 4.9, 7.4 Hz, 1 H), 7.39−7.35 (m, 1 H), 6.56 (s, 2 H), 4.78 (d, J = 5.5 Hz, 2 H), 4.45 (d, J = 5.6 Hz, 2 H), 4.32−4.28 (m, 1 H), 4.27−4.22 (m, 1 H), 1.66 (s, 3 H). MS m/z = 443.2 [M + H]$^+$. Calcd for $C_{25}H_{20}FN_4O_3$: 443.2.

■ ASSOCIATED CONTENT

Ⓢ Supporting Information

General information, experimental data and characterization, X-ray crystal structure information. This material is available free of charge via the Internet at http://pubs.acs.org.

Accession Codes

The PDB accession code for the X-ray cocrystal of BACE1 + compound **42** is 4RCD.

■ AUTHOR INFORMATION

Corresponding Author

*Phone: 617-444-5352. Fax: 617-621-3907. E-mail: tdineen@amgen.com. Address: Department of Medicinal Chemistry, Amgen Inc., 360 Binney Street, Cambridge, Massachusetts, United States.

Present Address

#For V.F.P.: Sanofi, 153 Second Avenue, Waltham, Massachusetts 02451, United States.

Author Contributions

The manuscript was written through contributions of all authors. All authors have given approval to the final version of the manuscript.

Notes

The authors declare no competing financial interest.

■ ABBREVIATIONS USED

AD, Alzheimer's disease; Aβ, β-amyloid; HEA, hydroxythethyl amine; APP, amyloid precursor protein; BACE, β-site APP cleaving enzyme; Pgp, P-glycoprotein

■ REFERENCES

(1) (a) Small, D. H.; Cappai, R. Alois Alzheimer and Alzeimer's Disease: A Centennial Perspective. *J. Neurochem.* **2006**, *99*, 708−710. (b) Goedert, M.; Spillantini, M. G. A century of Alzheimer's Disease. *Science* **2006**, *314*, 777−781. (b) Van Marum, R. J. Current and future therapy in Alzheimer's Disease. *Fundam. Clin. Pharmacol.* **2008**, *22*, 265−274. (c) Roberson, E. D.; Mucke, L. 100 Years and counting: prospects for defeating Alzheimer's Disease. *Science* **2006**, *314*, 781−784.

(2) (a) Catalano, S.; Dodson, E. C.; Henze, D. A.; Joyce, J. G.; Krafft, G. A.; Kinney, G. G. The role of amyloid-beta derived diffusible ligands (ADDLs) in Alzheimer's Disease. *Curr. Top. Med. Chem.* **2006**, *6*, 597−608. (b) Pimplikar, S. W. Reassessing the Amyloid Cascade Hypothesis of Alzheimer's Disease. *Int. J. Biochem. Cell Biol.* **2009**, *41*, 1261−1268.

(3) (a) Vassar, R.; Bennett, B. D.; Babu-Khan, S.; Kahn, S.; Mendiaz, E. A.; Denis, P.; Teplow, D. B.; Ross, S.; Amarante, P.; Loeloff, R.; Luo, Y.; Fisher, S.; Fuller, J.; Edenson, S.; Lile, J.; Jarosinski, M. A.; Biere, A. L.; Curran, E.; Burgess, T.; Louis, J. C.; Collins, F.; Treanor, J.; Rogers, G.; Citron, M. beta-Secretase cleavage of Alzheimer's amyloid precursor protein by the transmembrane aspartic protease BACE1. *Science* **1999**, *286*, 735−741. (b) Hussain, I.; Powell, D.; Howlett, D. R.; Tew, D. G.; Meek, T. D.; Chapman, C.; Gloger, I. S.; Murphy, K. E.; Southan, C. D.; Ryan, D. M.; Smith, T. S.; Simmons, D. L.; Walsh, F. S.; Dingwall, C.; Christie, G. Identification of a novel aspartic protease (Asp 2) as beta-secretase. *Mol. Cell. Neurosci.* **1999**, *14*, 419−427. (c) Yan, R.; Bienkowski, M. J.; Shuck, M. E.; Miao, H.; Tory, M. C.; Pauley, A. M.; Brashier, J. R.; Stratman, N. C.; Mathews, W. R.; Buhl, A. E.; Carter, D. B.; Tomasselli, A. G.; Parodi, L. A.; Heinrikson, R. L.; Gurney, M. E. Membraned-anchored aspartyl protease with Alzheimer's disease beta-secretase activity. *Nature* **1999**, *402*, 533−537. (d) Sinha, S.; Anderson, J. P.; Barbour, R.; Basi, G. S.; Caccavello, R.; Davis, D.; Doan, M.; Dovey, H. F.; Frigon, N.; Hong, J.; Jacobson-Croak, K.; Jewett, N.; Keim, P.; Knops, J.; Lieberburg, I.; Power, M.; Tan, H.; Tatsuno, G.; Tung, J.; Schenk, D.; Seubert, P.; Suomensaari, S. M.; Wang, S.; Walker, D.; Zhao, J.; McConlogue, L.; John, V. *Nature* **1999**, *402*, 537−540.

(4) Luo, X.; Yan, R. Inhibition of BACE1 for therapeutic use in Alzheimer's Disease. *Int. J. Clin. Exp. Pathol.* **2010**, *3*, 618−628.

(5) Johnsson, T.; Atwal, J. K.; Steinberg, S.; Snaedal, J.; Johnsson, P. V.; Bjornsson, S.; Stefansson, H.; Sulem, P.; Gudbjartsson, D.; Maloney, J.; Hoyte, K.; Gustafson, A.; Liu, Y.; Lu, Y.; Bhangale, T.; Graham, R. B.; Huttenlocher, J.; Bjornsdottir, G.; Andreassen, O. A.; Jönsson, E. G.; Palotie, A.; Behrens, T. W.; Magnusson, O. T.; Kong, A.; Thorsteinsdottir, U. A mutation in *APP* protects against Alzheimer's disease and age-related cognitive decline. *Nature* **2012**, *488*, 96−99.

(6) (a) Ghosh, A. K.; Shin, D.; Downs, D.; Koelsch, G.; Lin, X.; Ermolieff, J.; Tang, J. Design of potent inhibitors for human brainmemapsin 2 (β-secretase). *J. Am. Chem. Soc.* **2000**, *122*, 3522−3523. (b) Cumming, J. N.; Iserloh, U.; Kennedy, M. E. Design and development of BACE-1 inhibitors. *Curr. Opin. Drug Discovery Dev.* **2004**, *7*, 536−556. (c) Durham, T. B.; Shepherd, T. A. Progress toward the discovery and development of efficacious BACE inhibitors. *Curr. Opin. Drug Discovery Dev.* **2006**, *9*, 776−791. (d) Iserloh, U.; Wu, Y.; Cumming, J. N.; Pan, J.; Wang, L. Y.; Stamford, A. W.; Kennedy, M. E.; Kuvelkar, R.; Chen, X.; Parker, E. M.; Strickland, C.; Voigt, J. Potent pyrrolidine- and piperidine-based BACE-1 inhibitors. *Bioorg. Med. Chem. Lett.* **2008**, *18*, 414−417. (e) Iserloh, U.; Pan, J.; Stamford, A. W.; Kennedy, M. E.; Zhang, Q.; Zhang, L.; Parker, E. M.; McHugh, N. A.; Favreau, L.; Strickland, C.; Voigt, J. Discovery of an orally efficacious 4-phenoxypyrrolidine-based BACE-1 inhibitor. *Bioorg. Med. Chem. Lett.* **2008**, *18*, 418−422. (f) Clarke, B.; Demont, E.; Dingwall, C.; Dunsdon, R.; Faller, A.; Hawkins, J.; Hussain, I.; MacPherson, D.; Maile, G.; Matico, R.; Milner, P.; Mosley, J.; Naylor, A.; O'Brien, A.; Redshaw, S.; Riddell, D.; Rowland, P.; Soleil, V.; Smith, K.; Stanway, S. BACE-1 inhibitors part 2: identification of hydroxy ethylamines (HEAs) with reduced peptidic character. *Bioorg. Med. Chem. Lett.* **2008**, *18*, 1017−1022. (h) Charrier, N.; Clarke, B.; Cutler, L.;

Demont, E.; Dingwall, C.; Dunsdon, R.; Hawkins, J.; Howes, C.; Hubbard, J.; Hussain, I.; Maile, G.; Matico, R.; Mosley, J.; Naylor, A.; O'Brien, A.; Redshaw, S.; Rowland, P.; Soleil, V.; Smith, K.; Sweitzer, S.; Theobald, P.; Vesey, D.; Walter, D.; Wayne, G. Second generation of BACE-1 inhibitors. Part 1: The need for improved pharmacokinetics. *Bioorg. Med. Chem. Lett.* **2009**, *19*, 3664−3668. (i) Charrier, N.; Clarke, B.; Demont, E.; Dingwall, C.; Dunsdon, R.; Hawkins, J.; Hubbard, J.; Hussain, I.; Maile, G.; Matico, R.; Mosley, J.; Naylor, A.; O'Brien, A.; Redshaw, S.; Rowland, P.; Soleil, V.; Smith, K.; Sweitzer, S.; Theobald, P.; Vesey, D.; Walter, D.; Wayne, G. Second generation of BACE-1 inhibitors part 2: optimization of the non-prime side substituent. *Bioorg. Med. Chem. Lett.* **2009**, *19*, 3669−3673. (j) Charrier, N.; Clarke, B.; Cutler, L.; Demont, E.; Dingwall, C.; Dunsdon, R.; Hawkins, J.; Howes, C.; Hubbard, J.; Hussain, I.; Maile, G.; Matico, R.; Mosley, J.; Naylor, A.; O'Brien, A.; Redshaw, S.; Rowland, P.; Soleil, V.; Smith, K.; Sweitzer, S.; Theobald, P.; Vesey, D.; Walter, D.; Wayne, G. Second generation of BACE-1 inhibitors part 3: towards non-hydroxyethylamine transition state mimetics. *Bioorg. Med. Chem. Lett.* **2009**, *19*, 3674−3678. (k) Stachel, S. J. Progess toward the development of a viable BACE1 inhibitor. *Drug. Dev. Res.* **2009**, *70*, 101−110. and references therein. (i) Al-Tel, T. H.; Al-Qawasmeh, R. A.; Schmidt, M. F.; Al-Aboudi, A.; Rao, S. N.; Sabri, S. S.; Voelter, W. Rational design and synthesis of potent dibenzazepine motifs as β-secretase inhibitors. *J. Med. Chem.* **2009**, *52*, 6484−6488. (l) Cumming, J.; Babu, S.; Huang, Y.; Carrol, C.; Chen, X.; Favreau, L.; Greenlee, W.; Guo, T.; Kennedy, M.; Kuvelkar, R.; Le, T.; Li, G.; McHugh, N.; Orth, P.; Ozgur, L.; Parker, E.; Saionz, K.; Stamford, A.; Strickland, C.; Tadesse, D.; Voigt, J.; Zhang, L.; Zhang, Q. Piperazine sulfonamide BACE1 inhibitors: design, synthesis, and in vivo characterization. *Bioorg. Med. Chem. Lett.* **2010**, *20*, 2837−2842. (m) Al-Tel, T.; Semreen, M. H.; Al-Qawasmeh, R. A.; Schmidt, M. F.; El-Awadi, R.; Ardah, M.; Zaarour, R.; Rao, S. N.; El-Agnaf, O. Design, synthesis, and qualitative structure−activity evaluations of novel β-secretase inhibitors as potential Alzheimer's drug leads. *J. Med. Chem.* **2011**, *54*, 8873−8385. (m) Kaller, M. R.; Harried, S. S.; Albrecht, B.; Amarante, P.; Babu-Khan, S.; Bartberger, M. D.; Brown, J.; Brown, R.; Chen, K.; Cheng, Y.; Citron, M.; Croghan, M. D.; Dunn, R.; Graceffa, R.; Hickman, D.; Judd, T.; Kreiman, C.; La, D.; Lopez, P.; Luo, Y.; Masse, C.; Monenschein, H.; Nguyen, T.; Pennington, L. D.; San Miguel, T.; Wahl, R. C.; Weiss, M. M.; Wen, P. H.; Williamson, T.; Wood, S.; Xue, M.; Yang, B.; Zhang, J.; Patel, V.; Zhong, W.; Hitchcock, S. A potent and orally efficacious, hydroxyethylamine-based inhibitor of beta-secretase. *ACS Med. Chem. Lett.* **2012**, *3*, 886−891. (o) Weiss, M. M.; Williamson, T.; Babu-Khan, S.; Bartberger, M. D.; Brown, J.; Chen, K.; Cheng, Y.; Citron, M.; Croghan, M. D.; Dineen, T. A.; Esmay, J.; Graceffa, R. F.; Harried, S.; Hickman, D.; Hitchcock, S. A.; Horne, D. B.; Huang, H.; Imbeah-Ampiah, R.; Judd, T.; Kaller, M. R.; Kreiman, C. R.; La, D. S.; Li, V.; Lopez, P.; Louie, S.; Monenschein, H.; Nguyen, T. T.; Pennington, L. D.; Rattan, C.; San Miguel, T.; Sickmier, E. A.; Wahl, R. C.; Wen, P. H.; Wood, S.; Xue, Q.; Yang, B. H.; Patel, V. F.; Zhong, W. Design and preparation of a potent series of β-secretase inhibitors that demonstrate robust reduction of central β-amyloid. *J. Med. Chem.* **2012**, *55*, 9009−9024. (p) Dineen, T. A.; Weiss, M. M.; Williamson, T.; Acton, P.; Babu-Khan, S.; Bartberger, M. D.; Brown, J.; Chen, K.; Cheng, Y.; Citron, M.; Croghan, M. D.; Dunn, R. T.; Esmay, J.; Graceffa, R. F.; Harried, S. S.; Hickman, D.; Hitchcock, S. A.; Horne, D. B.; Huang, H.; Imbeah-Ampiah, R.; Judd, T.; Kaller, M. R.; Kreiman, C. R.; La, D. S.; Li, V.; Lopez, P.; Louie, S.; Monenschein, H.; Nguyen, T. T.; Pennington, L. D.; San Miguel, T.; Sickmier, E. A.; Vargas, H. M.; Wahl, R. C.; Wen, P. H.; Whittington, D. A.; Wood, S.; Xue, Q.; Yang, B. H.; Patel, V. F.; Zhong, W. Design and synthesis of potent, orally efficacious hydroxyethylamine derived β-site amyloid precursor protein cleaving enzyme (BACE1) inhibitors. *J. Med. Chem.* **2012**, *55*, 9025−9044. (q) Ng, R. A.; Sun; Mingua, S.; Bowers, S.; Hom, R. K.; Probst, G. D.; John, V.; Fang, L. Y.; Maillard, M.; Gailunas, A.; Brogley, L.; Neitz, R. J.; Tung, J. S.; Pleiss, M. A.; Konradi, A. W.; Sham, H. L.; Dappen, M. S.; Adler, M.; Yao, N.; Zmolek, W.; Nakamura, D.; Quinn, K. P.; Sauer, J.-M.; Bova, M. P.; Ruslim, L.; Artis, D. R.; Yednock, T. A. Design and synthesis of hydroxyethylamine (HEA) BACE-1 inhibitors: prime side chromane-containing inhibitors. *Biorg. Med. Chem. Lett.* **2013**, *23*, 4674−4679.

(7) (a) Congreve, M.; Aharony, D.; Albert, J.; Callaghan, O.; Campbell, J.; Carr, R. A. E.; Chessari, G.; Cowan, S.; Edwards, P. D.; Frederickson, M.; McMenamin, R.; Murray, C. W.; Patel, S.; Wallis, N. Application of fragment screening by X-ray crystallography to the discovery of aminopyridines as inhibitors of beta-secretase. *J. Med. Chem.* **2007**, *50*, 1124−1132. (b) Baxter, E. W.; Conway, K. A.; Kennis, L.; Bischoff, F.; Mercken, M. H.; Winter, H. L.; Reynolds, C. H.; Tounge, B. A.; Luo, C.; Scott, M. K.; Huang, Y.; Braeken, M.; Pieters, S. M.; Berthelot, D. J.; Masure, S.; Bruinzeel, W. D.; Jordan, A. D.; Parker, M. H.; Boyd, R. E.; Qu, J.; Alexander, R. S.; Brenneman, D. E.; Reitz, A. B. 2-Amino-3,4-dihydroquinazolines as inhibitors of BACE-1 (beta-site APP cleaving enzyme): use of structure based design to convert a micromolar hit into a nanomolar lead. *J. Med. Chem.* **2007**, *50*, 4261−4264. (c) Barrow, J.; Rittle, K.; Ngo, P.; Selnick, H.; Graham, S.; Pitzenberger, S.; McGaughey, G.; Colussi, D.; Lai, M.-T.; Huang, Q.; Tugusheva, K.; Espeseth, A.; Simon, A.; Munshi, S.; Vacca, J. Design and synthesis of 2,3,5-substituted imidazolidin-4-one inhibitors of BACE-1. *ChemMedChem* **2007**, *2*, 995−999. (d) Malamas, M. S.; Erdei, J.; Gunawan, I.; Barnes, K.; Johnson, M.; Hui, Y.; Turner, J.; Hu, Y.; Wagner, E.; Fan, K.; Olland, A.; Bard, J.; Robichau, A. J. Aminoimidazoles as potent and selective human β-secretase (BACE1) inhibitors. *J. Med. Chem.* **2009**, *52*, 6314−6323. (e) Malamas, M. S.; Erdei, J.; Gunawan, I.; Turner, J.; Hu, Y.; Wagner, E.; Fan, K.; Chopra, R.; Olland, A.; Bard, J.; Jacobsen, S.; Magolda, R. L.; Pangalos, M.; Robichaud, A. J. Design and synthesis of 5,5′-disubstituted aminohydantoins as potent and selective human β-secretase (BACE1) inhibitors. *J. Med. Chem.* **2010**, *53*, 1146−1158. (f) May, P. C.; Dean, R. A.; Lowe, S. L.; Martenyi, F.; Sheehan, S. M.; Boggs, L. N.; Monk, S. A.; Mathes, B. M.; Mergott, D. J.; Watson, B. M.; Stout, S. L.; Timm, D. E.; LaBell, E. S.; Gonzales, C. R.; Nakano, M.; Jhee, S. S.; Yen, M.; Ereshefsky, L.; Lindstrom, T. D.; Calligaro, D. O.; Cocke, P. J.; Hall, D. G.; Friedrich, S.; Citron, M.; Audia, J. E. Robust central reduction of amyloid-β in humans with an orally available, non-peptidic β-secretase inhibitor. *J. Neurosci.* **2011**, *31*, 16507−16516. (g) Swahn, B.; Holenz, J.; Kihlstrom, J.; Kolmodin, K.; Lindstrom, J.; Plobeck, N.; Rotticci, D.; Sehgelmeble, F.; Sundstrom, M.; Berg, S. v.; Falting, J.; Georgievska, B.; Gustavsson, S.; Neelissen, J.; Ek, M.; Olsson, L.; Berg, S. Aminoimidazoles as BACE-1 inhibitors: the challenge to achieve in vivo brain efficacy. *Bioorg. Med. Chem. Lett.* **2012**, *22*, 1854−1859. (h) Gravenfors, Y.; Viklund, J.; Blid, J.; Ginman, T.; Karlström, S.; Kihlström, J.; Kolmodin, K.; Lindström, J.; von Berg, S.; von Kieseritzky, F.; Slivo, C.; Swahn, B.-M.; Olsson, L.-L.; Johansson, P.; Eketjäll, S.; Fälting, J.; Jeppsson, F.; Strömberg, K.; Janson, J.; Rahm, F. New aminoimidazoles as β-secretase (BACE-1) inhibitors showing amyloid-β (Aβ) lowering in brain. *J. Med. Chem.* **2012**, *55*, 9297−9311. (i) Mandal, M.; Zhu, Z.; Cumming, J. N.; Liu, X.; Strickland, C.; Mazzola, R. D.; Caldwell, J. P.; Leach, P.; Grzelak, M.; Hyde, L.; Zhang, Q.; Terracina, G.; Zhang, L.; Chen, X.; Kuvelkar, R.; Kennedy, M. E.; Favreau, L.; Cox, K.; Orth, P.; Buevich, A.; Voigt, J.; Wang, H.; Kazakevich, I.; McKittrick, B. A.; Greenlee, W.; Parker, E. M.; Stamford, A. W. Design and validation of bicyclic iminopyrimidinones as beta amyloid cleaving enzyme-1 (BACE1) inhibitors: conformational constraint to favor a bioactive conformation. *J. Med. Chem.* **2012**, *55*, 9331−9345. (j) Stamford, A. W.; Scott, J. D.; Li, S. W.; Babu, S.; Tadesse, D.; Hunter, R.; Wu, Y.; Misiaszek, J.; Cumming, J. N.; Gilbert, E. J.; Huang, C.; McKittrick, B. A.; Hong, L.; Guo, T.; Zhu, Z.; Strickland, C.; Orth, P.; Voigt, J. H.; Kennedy, M. E.; Chen, X.; Kuvelkar, R.; Hodgson, R.; Hyde, L. A.; Cox, K.; Favreau, L.; Parker, E. M.; Greenlee, W. J. Discovery of an orally available, brain penetrant BACE1 inhibitor that affords robust CNS Aβ reduction. *ACS Med. Chem. Lett.* **2012**, *3*, 897−902.

(8) Huang, H.; La, D. S.; Cheng, A. C.; Whittington, D. A.; Patel, V. F.; Chen, K.; Dineen, T. A.; Epstein, O.; Graceffa, R.; Hickman, D.; Kiang, Y.-H.; Louie, S.; Lou, Y.; Wahl, R. C.; Wen, P. H.; Wood, S.; Fremeau, R. T., Jr. Structure- and property-based design of aminooxazoline xanthenes as selective, orally efficacious, and CNS

penetrable BACE inhibitors for the treatment of Alzheimer's disease. *J. Med. Chem.* **2012**, *55*, 9156−9169.
(9) Epstein, O.; Bryan, M. C.; Cheng, A. C.; Derakhchan, K.; Dineen, T. A.; Hickman, D.; Hua, Z.; Human, J. B.; Kreiman, C. E.; Marx, I. E.; Weiss, M. M.; Qu, Y.; Wahl, R. C.; Wen, P. H.; Whittington, D. A.; Wood, S.; Zheng, X. M.; Fremeau Jr., R. T.; White, R. D.; Patel, V. F. Lead optimization and modulation of hERG activity in a series of aminooxazoline xanthene BACE inhibitors. *J. Med. Chem.* **2014**, *57*, DOI: 10.1021/jm501266w.
(10) (a) Mahar Doan, K. M.; Humphreys, J. E.; Webster, L. O.; Wring, S. A.; Shampine, L. J.; Serabjit-Singh, C. J.; Adkinson, K. K.; Polli, J. W. Passive permeability and P-glycoprotein mediated efflux differentiate CNS and non-CNS marketed drugs. *J. Pharmacol. Exp. Ther.* **2002**, *303*, 1029−1037. (b) Hitchcock, S. A.; Pennington, L. D. Structure−brain exposure relationships. *J. Med. Chem.* **2006**, *49*, 7559−7583.
(11) Bissantz, C.; Kuhn, B.; Stahl, M. A medicinal chemist's guide to molecular interactions. *J. Med. Chem. 53*, 5061−5084.
(12) (a) Hassner, A.; Lorber, M. E.; Heathcock, C. Addition of iodine isocyanate to olefins. Scope and synthetic utility. *J. Org. Chem.* **1967**, *32*, 540−549. (b) Fernandez, J. M. G.; Mellet, C. O.; Adrian, M. A. P.; Mota, J. F. Syntheses and spectral properties of β-iodoureas and 2-amino-4,4-diphenyl-2-oxazolines. *J. Heterocycl. Chem.* **1991**, *28*, 777−780.
(13) For a review, see Miyaura, N.; Suzuki, A. Palladium-catalyzed cross-coupling reactions of organoboron compounds. *Chem. Rev.* **1995**, *95*, 2456−2483.
(14) (a) Fernandez, D.; Ghanta, A.; Kauffman, G. W.; Sanguinetti, M. C. Physicochemical features of the hERG channel drug binding site. *J. Biol. Chem.* **2004**, *279*, 10120−10127. (b) Jamieson, C.; Moir, E. M.; Rankovic, Z.; Wishart, G. Medicinal chemistry of hERG optimizations: highlights and hang-ups. *J. Med. Chem.* **2006**, *49*, 5029−5046.
(15) Seelig, A.; Landwojtowicz, E. Structure−activity relationship of P-glycoprotein substrates and modifiers. *Eur. J. Pharm. Sci.* **2000**, *12*, 31−40.
(16) Coordinates for the complex of BACE1 with inhibitor **42** have been deposited in the Protein Data Bank under PDB 4RCD.
(17) Riley, R. J.; Grime, K.; Weaver, R. Time-dependent CYP inhibition. *Expert Opin. Drug Metab. Toxicol.* **2007**, *3*, 51−66 and references therein..
(18) Berry, L. M.; Zhao, Z. An Examination of IC_{50} and IC_{50}-shift experiments in assessing time-dependent inhibition of CYP3A4, CYP2D6, and CYP2C9 in human liver microsomes. *Drug. Metab. Lett.* **2008**, *8*, 51−59.
(19) In general, aminoxazoline xanthene compounds displayed similar PK profiles in rats and maximum effects on Aβ reduction in the CSF and brain were observed between 4 and 5 h following an oral dose in the PD assay.
(20) (a) Lin, J. H. CSF as a surrogate for assessing CNS exposure: an industrial perspective. *Curr. Drug Metab.* **2008**, *9*, 46−59. (b) Liu, X.; Van Natta, K.; Yeo, H.; Vilenski, O.; Weller, P. E.; Worboys, P. D.; Monshouwer, M. Unbound drug concentration in brain homogenate and cerebral spinal fluid at steady state as a surrogate for unbound concentration in brain interstitial fluid. *Drug. Metab. Dispos.* **2009**, *37*, 787−793.
(21) Felmlee, M. A.; Morris, M. E.; Mager, D. E. Mechanism-based pharmacodynamic modeling. *Methods Mol. Biol.* **2012**, *929*, 583−600.
(22) Finlayson, K.; Turnbull, L.; January, C. T.; Sharkey, J.; Kelly, J. S. [^{3}H]Dofetilide binding to HERG transfected membranes: a potential high throughput preclinical screen. *Eur. J. Pharmacol.* **2001**, *430*, 147−148.